SELF-STEERING ARRAYS FOR WIRELESS COMMUNICATION NETWORKS

A THESIS SUBMITTED TO THE GRADUATE DIVISION OF THE UNIVERSITY OF HAWAI'I IN PARTIAL FULFILLMENT OF THE REQUIREMENTS FOR THE DEGREE OF

MASTER OF SCIENCE

IN

ELECTRICAL ENGINEERING

AUGUST 2004

By
Grant S. Shiroma

Thesis Committee

Wayne A. Shiroma, Chairperson
Ryan Y. Miyamoto
Eric L. Miller

ACKNOWLEDGMENTS

I would like to first acknowledge Dr. Wayne Shiroma for his guidance and encouragements throughout both my undergraduate and graduate studies. This work would not have been possible without him as his dedication to the success of his students goes far beyond the classroom and is simply unsurpassed.

Next, I would like to thank Dr. Eric Miller for all of his support and for having such a great attitude towards education and engineering. A special thanks to Dr. Ryan Miyamoto and Dr. Jussi Tuovinen for their guidance in my research. My education has been greatly enriched by their knowledge and experiences. Thanks to the past members of the MMRL research group for setting an example with high standards for others to follow. To the present members of the MMRL group, especially Blaine Murakami, Justin Roque, and Stephen Sung, who continue to raise the standard, thank you for all of your hard work, support, and encouragement. I am confident that the MMRL group will continue to succeed in your presence.

I am also grateful to the National Science Foundation and the Air Force Office of Scientific Research for supporting my research during the past 2 years.

Finally, I would like to give a special thanks to my family and friends for their continuing support.

ABSTRACT

A Retrodirective array has the unique property in that when it is interrogated, the array automatically points its beam toward the interrogator. Unlike more complicated arrays that require digital signal processing, the retrodirective array achieves self-steering through simple analog circuits. As a result, retrodirective arrays are the preferred solution for applications requiring self-steering where the limiting factors are cost and design complexity.

This thesis presents several advances in wireless communications systems through the use of retrodirective arrays. First, a phase-conjugating retrodirective array is used to improve the reliability of a radio link in a severe multipath environment. The method showed up to 31 dB of improvement of a 5.35-GHz communication system when compared to a conventional array. Next, for terrestrial-to-space or space-to-space applications, a two-dimensional retrodirective array is presented at 3.84 GHz. The complexity of a complicated LO feed network is eliminated by basing the design on self-oscillating mixers. Finally, a retrodirective array is specifically designed for a 10.5-GHz small-satellite network. A network of small satellites promise increased mission flexibility and success by distributing the tasks of a single large satellite. Quadruple subharmonic mixing is used as well as two-dimensional retrodirectivity and circular polarization to accommodate for the power constraints and lack of attitude control of small satellites.

TABLE OF CONTENTS

LIST OF FIGURES

CHAPTER 1

INTRODUCTION

Wireless communication devices such as cell phones, wireless internet, and satellite communications have revolutionized the day-to-day operations of businesses, the military, and the everyday person. These inventions, once seen as luxuries, are now becoming a part of modern-day life fueling a wireless industry that shows no signs of slowing down. Within a five-year span, net sales for Nokia, a leader in cell phones and other wireless communication devices, have jumped from $16.4 million in 1998 to $36.2 million in 2003, which is nearly the all-time high of $37.3 million [1].

Research spending at Nokia is also at an all-time high of $4.6 million in 2003, more than triple the amount in 1998. No longer are wireless devices being designed just for audio communication. Some of the latest technologies include portable video imaging and gaming systems with online capabilities. With the popularity of wireless communication systems likely to increase in the future, many opportunities will open in the field to support the growing demand.

While state-of-the-art wireless communication systems are comprised of many different subsystems and components, the focus on this thesis is the antenna. More specifically, new designs of retrodirective arrays will be discussed along with their beneficial properties to a wireless system.

1.1 Omnidirectional Antennas

The ability of an antenna to convert electric signals to electromagnetic waves which propagate in space is what allows the transfer of information from one point to another. Omnidirectional antennas, as shown in Fig. 1.1, are the simplest and most

common type of antennas used in wireless communication systems. They are cost effective, as they may consist of only a single wire, and provide good coverage equally in all directions. As a result, each user does not have to know the location of the base station antenna to establish contact.

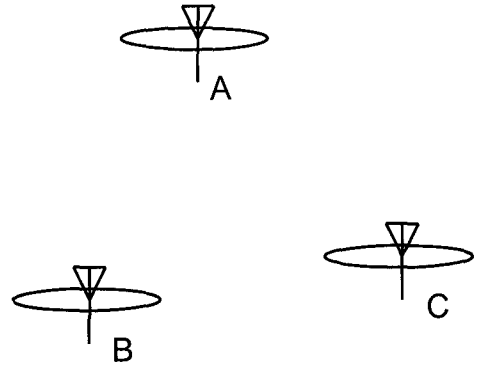

Fig. 1.1. Wireless network using omnidirectional antennas.

While omnidirectional antennas may be adequate for commercial applications where cost is the limiting factor, there are some downsides of using an antenna that has such a broad radiation pattern. When transmitting, power is radiated in all directions which is both inefficient and may cause interference to other systems. For the receiving case, in addition to receiving the desired signal, an omnidirectional antenna may also pick up interference coming from users in other directions. Interference can be avoided between two neighboring stations by assigning different frequencies to different users, forming a frequency division multiplexing (FDM) network. However, with all of the frequencies between 9 kHz - 300 GHz currently allocated [2], available bandwidth is starting to become one of the major limiting factors in the development of future, high performance wireless systems. Also, since it is possible that some communications may contain sensitive information, transmitting the information in all directions using omnidirectional antennas may create a security issue.

1.2 Phased Arrays

The easiest way to increase the radiation efficiency of a wireless system is to transmit only in the direction of the desired user. Not only does this increase the radiation efficiency, but it also reduces interference to other users which increases capacity as well as security. This method of increasing the user capacity by only transmitting to selected areas is known as space division multiplexing (SDM).

One way of realizing an SDM network is through the use of phased arrays as shown in Fig. 1.2. Each antenna element in the array is connected to a phase shifter which allows beam steering of the array. Once the direction of the user is known, the beam can be pointed towards that user (user A), increasing the radiation efficiency of the system while minimizing interference in other direction (user B). The problem with phased arrays is that the location of the user must be predetermined, making it unsuitable for mobile users.

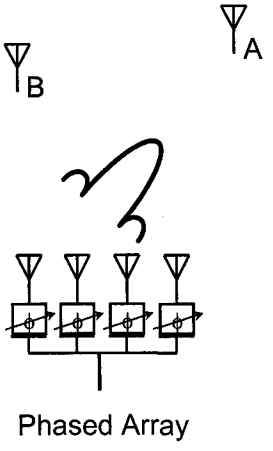

Fig. 1.2. Wireless network using phased arrays.

1.3 Smart Antenna

The preferred solution for mobile users in a SDM network is to use an array equipped with self-steering capabilities. One popular type of antenna capable of self-steering is the digitally based smart antenna [3]. The smart antenna (Fig. 1.3) downconverts the RF signal to baseband where digital signal processing (DSP) algorithms are applied to determine the directions of the users and in turn, form a beam back in that direction. Advanced algorithms can perform complicated functions such as compensate for multipath fading and, by analyzing both the direct and multipath signals, selectively receive and transmit to multiple sources (desired or interference). However, due to the added cost and complexity of a DSP system, in additional to the analog downconversion circuit, the smart antenna may not be suitable for all applications.

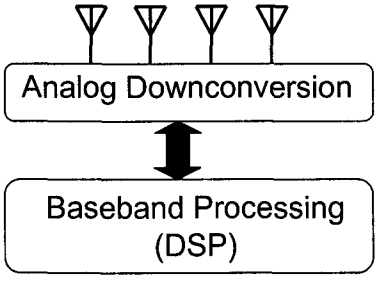

Fig. 1.3. Schematic of a smart antenna system.

1.4 Retrodirective Arrays

This thesis will focus on retrodirective arrays which is the preferred solution for applications requiring self-steering where the limiting factors are cost and design complexity. Retrodirective arrays have the unique property in that when the array is interrogated, the array automatically points its beam toward the interrogator. Unlike the smart antenna which relies on DSP algorithms, retrodirective arrays achieve self-steering completely through simple analog circuits. The phase-conjugating retrodirective array

(Fig. 1.4) uses an analog phase conjugator, typically a heterodyne mixer [4], to achieve self-steering. The benefits include those of a phased array such as increased link efficiency, added security, and increased user capacity, as well as automatic tracking, with minimal added complexity.

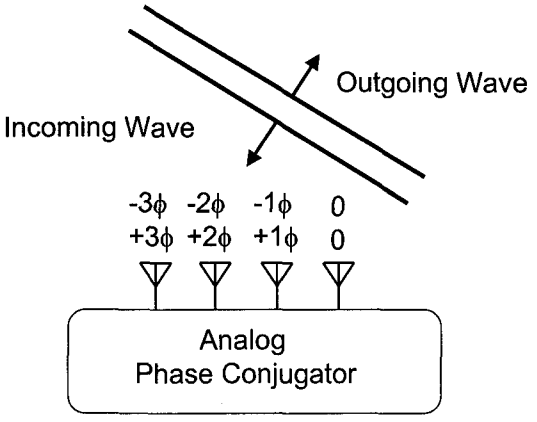

Fig. 1.4. Schematic of a phase-conjugating retrodirective array.

1.4.1 Multipath Communication Using Retrodirective Arrays

Multipath propagation of a communication signal is one of the leading causes of fading and loss of connections between two wireless users. As shown in Fig. 1.5, in addition to the direct propagation path, the signal also reaches the destination through a second path. Depending on the relative distances between these two paths, the resultant signal may either add in-phase (no loss of communication), or out–of-phase (complete loss of communication). In reality, the multipath signals combine somewhere between in-phase and out-of-phase resulting in some degree of fading.

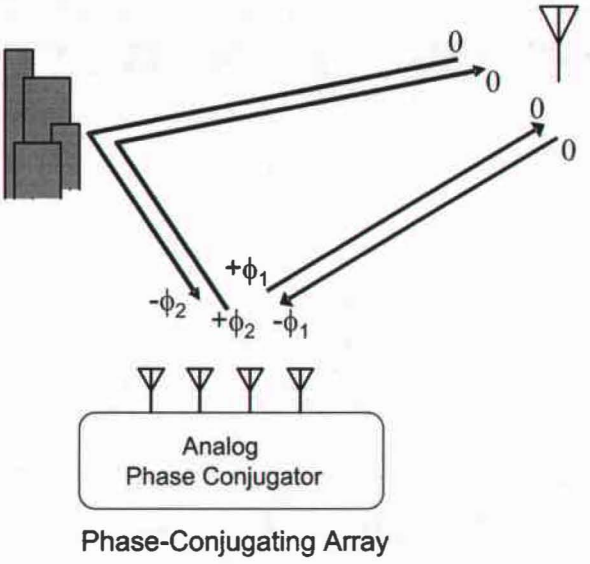

Fig. 1.5. Wireless communication with multipath propagation using a phase-conjugating array.

Chapter 3 discusses how a phase-conjugating retrodirective array can be used to reduce multipath fading. In the ideal case, multipath fading can be completely eliminated. If the resulting phases of the two incoming multipath signals are $-\phi_1$ and $-\phi_2$, the phase conjugating array will transmit the phase conjugate $+\phi_1$ and $+\phi_2$. Back at the original source, these two signals from the phase conjugating array will combine in-phase, thus eliminating the deep fading due to multipath.

1.4.2 Retrodirective Arrays for Non-Terrestrial Communication

While 1D steering is adequate for terrestrial to terrestrial communications, two-dimensional (2D) steering is required for terrestrial to space (Fig. 1.6) or space to space applications.

In the case of the retrodirective array, the challenge is to reduce the size of the design to a half-wavelength by half-wavelength unit cell. The smaller size not only aids

Fig. 1.6. Two-dimensional self-steering array for non-terrestrial communication.

installation, but also eliminates the grating lobes. Conventional phase-conjugating arrays employ heterodyne mixers at each element that are fed by a single local oscillator (LO) source through a large corporate feed network. Chapter 4 proposes a design that will eliminate the complicated feed network by replacing the mixers with self-oscillating mixers. Basing the design of the array on self-oscillating mixers allows each element to be self-contained within a half wavelength by half wavelength unit cell.

1.4.3 Retrodirective Arrays for Small-Satellite Networks

Recently, there has been considerable interest in small satellites for environmental sensing, technology demonstrations, and other short-development experiments [5]. The smaller mass of nanosatellites (10 kg) and picosatellites (1 kg) make them more economical to develop and launch into orbit. Networks of small satellites promise increased mission flexibility and success by distributing the tasks and subsystems typical of a single large satellite. An autonomous small-satellite network also reduces the possibility of catastrophic single-point failure; if one picosatellite fails, others can take up the slack until a replacement is launched. However, the challenge in

designing a distributed small-satellite network – especially a dynamically reconfigurable one – is in establishing and maintaining a reliable crosslink with other satellites in the network without *a priori* knowledge of their positions.

The 10 x 10 x 15 cm size of picosatellites prohibits them from having attitude control. Therefore, there is an added challenge of maintaining a reliable link with satellites that are constantly moving in space. Self-steering arrays can increase the communication efficiency of a small-satellite network due to the added gain of the array as well as provide an additional layer of security. Due to the size constraints and limited DC power, the retrodirective array is the preferred choice over the more complicated smart antenna because it requires no DSP layer.

Chapter 5 presents a design of a retrodirective array, specifically for picosatellite applications. The proposed design utilizes a novel quadruple subharmonic mixing approach to lower the LO frequency requirement, in addition to achieving two-dimensional retrodirectivity with circular polarization.

1.5 Organization of the Thesis

Chapter 2 discusses the various types of retrodirective arrays and how they are characterized. First, the corner reflector is introduced as a physical interpretation of a self-steering device. Next, the Van Atta array and phase-conjugating arrays are discussed, followed by design examples. Finally, the method of characterizing retrodirective arrays with bistatic and monostatic radiation patterns are discussed, along with the theoretical analysis.

A method of using phase-conjugating arrays to increase the reliability of a wireless link in a severe multipath environment is introduced in Chapter 3. An experimental setup is built to verify the method.

The problems of physically implementing a two-dimensional phase-conjugating retrodirective array are addressed in Chapter 4. The proposed solution replaces the conventional heterodyne mixers with self-oscillating mixers.

Chapter 5 discusses one of the most promising applications of retrodirective arrays. Retrodirective arrays are designed to provide secure crosslinks in an autonomous network of small satellites. The design specifically accounts for the space and DC power limitations of the satellite by utilizing a quadruple subharmonic mixing approach. Two-dimensional retrodirectivity and circular polarization is also achieved.

Finally, general conclusions and areas of further research are discussed in Chapter 6.

CHAPTER 2

RETRODIRECTIVE ARRAYS

Chapter 1 discussed how the self-steering properties of retrodirective arrays can be used to increase the link efficiency and security of a wireless system. The first half of Chapter 2 begins by discussing the fundamentals of retrodirective array design. First, the corner reflector is introduced as a physical incite into retrodirectivity. Then, the Van Atta array is discussed. The operation of the phase-conjugating array is explained next, along with examples of a 4-element prototype array using a spatially fed LO and a retrodirective array capable of full-duplex communication.

Methods of characterizing retrodirective arrays are discussed in the second half of Chapter 2. Since retrodirective arrays are self-phasing phased arrays, a theoretical background is built around a phased array of isotropic radiators. The analysis then proceeds by including the effects of microstrip patch antennas as the array elements. Finally, the retrodirective array is characterized through bistatic and monostatic radiation patterns.

2.1 Types of Retrodirective Arrays

2.1.1 Corner Reflector

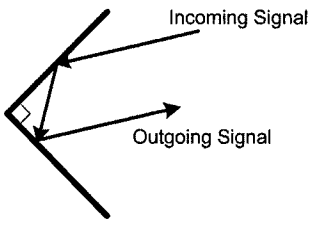

Fig. 2.1. 90° Corner reflector.

The 90° corner reflector [6] is the simplest example of a retrodirective device. As shown in Fig. 2.1, orthogonal metal plates reflect an incoming signal back in the direction it originated. A relatively large size is required to minimize the effect of edge diffraction which distorts the retrodirected radiation pattern. Although well-suited for applications such as radar targets or markers, the large size and difficulty in integrating electronics make corner reflectors unsuitable for wireless communications.

2.1.2 Van Atta Array

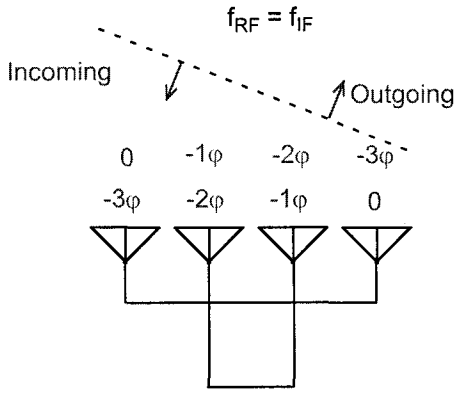

Fig. 2.2. Van Atta array.

Another way of achieving retrodirectivity is through the use of Van Atta arrays [7]. As shown in Fig. 2.2, the Van Atta array consists of pairs of antenna elements equally spaced from the center with equal-length lines. The progressive phase shift associated with the incoming signal is phase-lagged (from right-to-left) across the array. The arrangement of the array causes a reversal of this phase progression for the outgoing signal, resulting in its reflection back in the originating direction. As the lengths of the transmission lines are physically equal, the only frequency-dependent component in the Van Atta array is the antenna. The use of broadband antennas and non-dispersive transmission lines allows the array to transpond broadband signals.

The simple topology of a Van Atta array has lead to the design of the highest frequency active retrodirective array at 66 GHz [8]. The disadvantage of the Van Atta array is that the incoming wave must be planar to achieve retrodirectivity.

2.1.3 Phase-Conjugating Array

A third way of achieving retrodirectivity is through phase conjugation. As shown in Fig. 2.3, an incoming plane wave will induce a progressive phase delay φ to each element from right to left. If the phase of the outgoing wave is conjugated, such that the element on the left is excited first, the retransmitted signal will be in the direction of the original source.

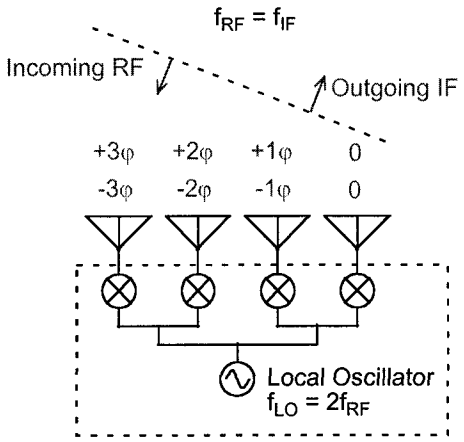

Fig. 2.3. Phase conjugating array using heterodyne mixers.

The phase-conjugating circuitry is typically comprised of heterodyne mixers [4] where the incoming radio-frequency (RF) signal at each element is mixed with a synchronized local-oscillator (LO) signal at twice the RF frequency. The mixing process results in an intermediate-frequency (IF) signal that contains a phase-conjugated copy of the original RF signal.

An intuitive understanding of frequency generation in a heterodyne mixer, as described in [9], can be obtained by analyzing the simplified circuit of a diode and voltage source as shown in Fig. 2.4(a).

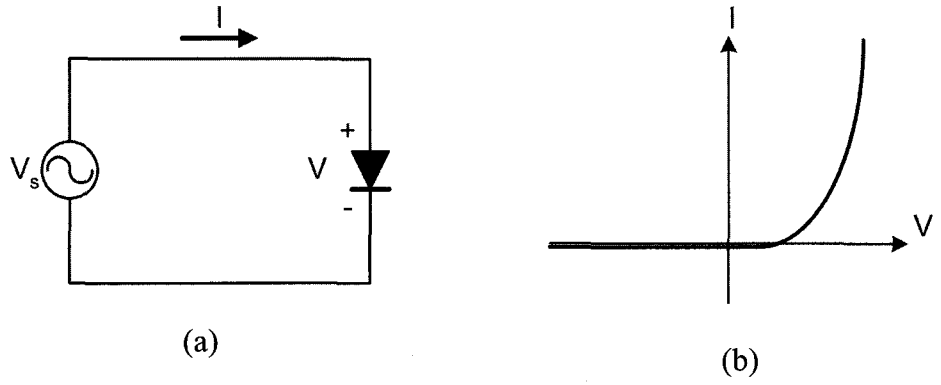

Fig. 2.4. (a) Simplified diode mixer circuit of a diode connected to voltage source. (b) Typical I/V characteristic of diode.

The exponential *I/V* characteristics of the diode (Fig. 2.4(b)) can be expressed as a power series

$$I = aV + bV^2 + cV^3 + \cdots \tag{2.1}$$

where *a*, *b*, and *c* are the power series coefficients and are unique to a specific diode. If V_s is the sum of the RF and LO signals,

$$V_s = V_1 \cos(\omega_{LO} t) + V_2 \cos(\omega_{RF} t + \varphi) \tag{2.2}$$

by substituting (2.2) into (2.1), the first term is

$$I_a = aV_1 \cos(\omega_{LO} t) + aV_2 \cos(\omega_{RF} t + \varphi) \tag{2.3}$$

After simplifying, the second term is

$$I_b = \frac{b}{2}\{V_1^2 + V_2^2 + V_1^2 \cos(2\omega_{LO} t) + V_2^2 \cos(2\omega_{RF} t + 2\varphi) \tag{2.4}$$

$$+ 2V_1 V_2 [\cos((\omega_{LO} + \omega_{RF})t + \varphi) + \cos((\omega_{LO} - \omega_{RF})t - \varphi)]\}$$

If the LO frequency is twice the RF frequency, $\omega_{LO} = 2\omega_{RF}$, the sum of (2.3) and (2.4) becomes

$$I_{a+b} = \frac{b}{2}\left(V_1^{\,2} + V_2^{\,2}\right) + aV_2\cos(\omega_{RF}t + \phi) + bV_1V_2\cos(\omega_{RF}t - \phi) \qquad (2.5)$$
$$+ aV_1\cos(2\omega_{RF}t) + \frac{bV_2^{\,2}}{2}\cos(2\omega_{RF}t + 2\phi)$$
$$+ bV_1V_2\cos(3\omega_{RF}t + \phi) + \frac{bV_1^{\,2}}{2}\cos(4\omega_{RF}t)$$

which reveals the phase conjugated term,

$$V_2\cos(\omega_{RF}t + \varphi)^* = bV_1V_2\cos(\omega_{RF}t - \phi) \qquad (2.6)$$

The higher frequency terms can be filtered out and a balanced circuit [10] is used to suppress the remaining $aV_2\cos(\omega_{RF}t + \phi)$ RF leakage term. Following, are two examples of prototype retrodirective array circuits.

A four-element phase conjugating array using FET mixers is shown in Fig. 2.5 [11]. The incoming RF and outgoing IF signals utilize two separate cross-polarized patch antennas, while the LO signal is fed spatially to an antenna on the back of the array. The RF and LO are combined and fed to the gate of the FET via a diplexer. The phase conjugated IF is taken off of the drain terminal.

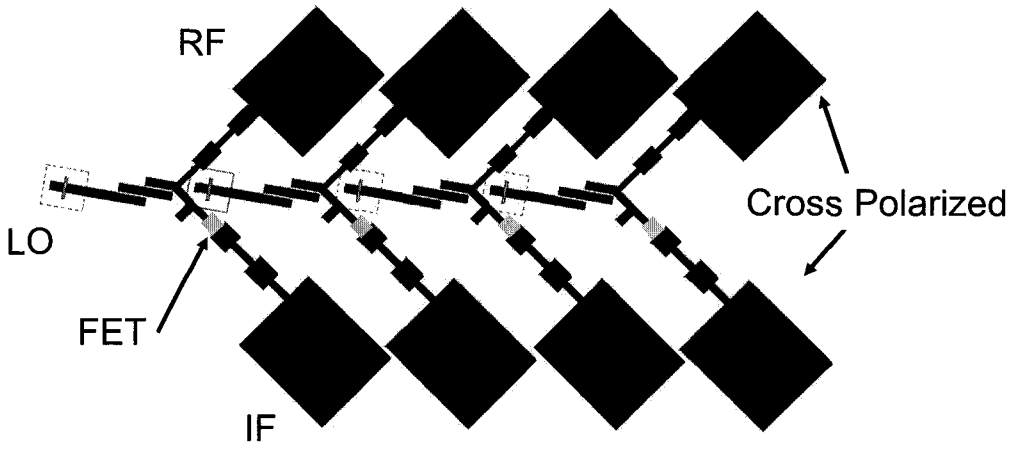

Fig. 2.5. Four-element phase-conjugating array using FET mixers [11].

To enable duplex retrodirective communication, it is necessary for a retrodirective array to have a receiver function in addition to the transponder function. A full-duplex retrodirective array system has developed at the University of Michigan [12]. Each phase conjugator employs two mixers. The frequency of the LO applied to the first mixer is slightly higher than that of the incoming RF signal. This mixing process generates a low-frequency phase-conjugated IF signal, which then proceeds to a carrier/data recovery circuit followed by a BPSK modulator. The output signal is upconverted by the second mixer and transmitted, and the recovered data is processed by an A/D converter. The carrier-recovery system allows the retrodirective array to use the modulated RF signal as an interrogating RF signal, enabling full-duplex retrodirective array communications. Using a 78.125-kbps data rate, a full-duplex data transmission test resulted in a bit error rate of better than 10^{-6} for 10-dB signal-to-noise ratios without error correction.

2.2 Characterization of Retrodirective Arrays

Retrodirective arrays are characterized by their bistatic and monostatic radiation patterns. Since these patterns are a function of both the element factor and the array factor, they will be explained by first considering a phased array of isotropic elements. Then the effect of using microstrip patch antennas will be considered, followed by the self-phasing property of the retrodirective array.

2.2.1 Phased Arrays with Isotropic Elements

A first step in analyzing an antenna array is to assume that the antenna elements are isotropic radiators (i.e. radiate equally in all directions). This simplifies the result to include only the effects of the array, or the "array factor", without the influence of the antenna element or "element factor." The element factor is later multiplied with the array factor to obtain the overall radiation pattern.

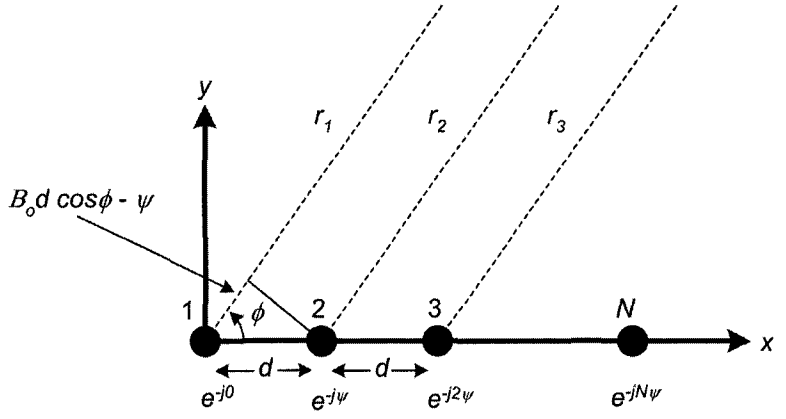

Fig. 2.6. Antenna array with isotropic antenna elements.

Fig. 2.6 is an array of N isotropic radiators aligned on the x-axis and spaced a distance d apart. Each element is fed with the same amplitude but with phase progression ψ from left to right.

The radiation pattern of the array is found by examining the total electric field generated by the sum of all the elements in the array as described in [13]. For the electric field to add in phase at the direction ϕ, there must be a phase difference of

$$\beta_o d\cos\phi - \psi \tag{2.7}$$

between elements. Under far-field approximations, the array factor is then the sum of the electric fields from each element:

$$AF = 1 + e^{j(\beta_o d\cos\phi - \psi)} + e^{j2(\beta_o d\cos\phi - \psi)} + \cdots + e^{j(N-1)(\beta_o d\cos\phi - \psi)} \tag{2.8}$$

Simplifying and normalizing (2.8) yields the normalized array factor,

$$\left|AF\right|_n = \frac{1}{N}\frac{\sin\frac{N}{2}(\beta_o d\cos\phi - \psi)}{\sin\frac{1}{2}(\beta_o d\cos\phi - \psi)} \tag{2.9}$$

Fig. 2.7 is a plot of the radiation patterns of an $N = 4$ element array where the isotropic antenna elements are spaced $\lambda/2$ apart. By setting $\psi = 0°$, $45°$, $-90°$, and $180°$ in (2.9), the peak of the main lobe shifts to $\phi = 90°$, $75.5°$, $120°$, and $180°$, respectively.

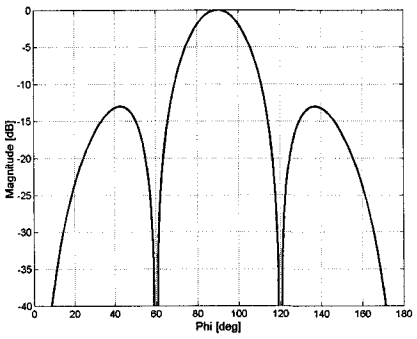

(a)

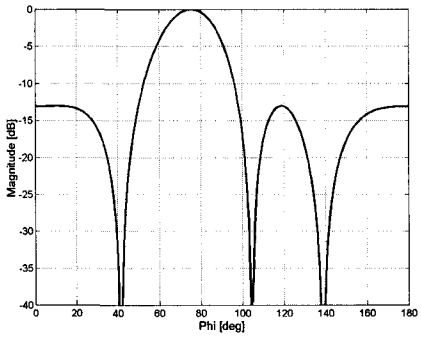

(b)

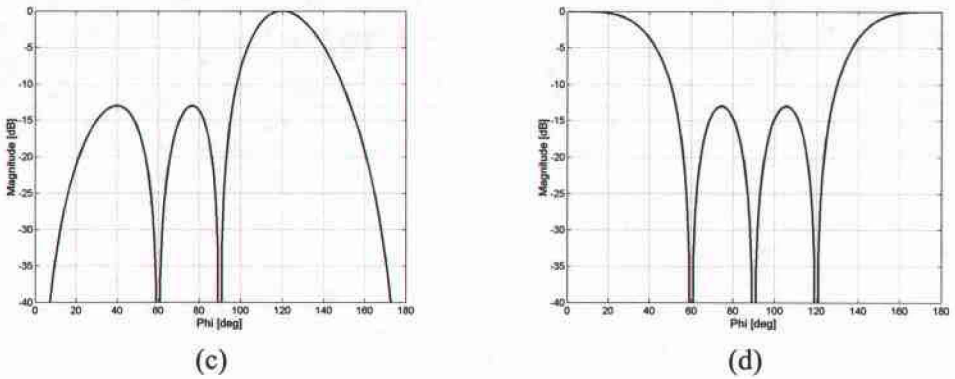

Fig. 2.7. Radiation pattern of a 4-element array using isotropic elements spaced λ/2: (a) ψ = 0°, (b) ψ = 45°, (c) ψ = -90°, (d) ψ = 180°. The peak of the main lobe is shifted to $\phi = 90°, 75.5°, 120°$, and $180°$ respectively.

2.2.2 Phased Arrays with Patch Antenna Elements

While an isotropic radiator is useful for the theoretical analysis of arrays, it does not exist in practice. At microwave frequencies, antenna arrays are commonly built around the microstrip patch antenna. Its low profile, simple design, and ability to be fabricated on the same substrate as the circuit make it very popular in both prototype and production designs.

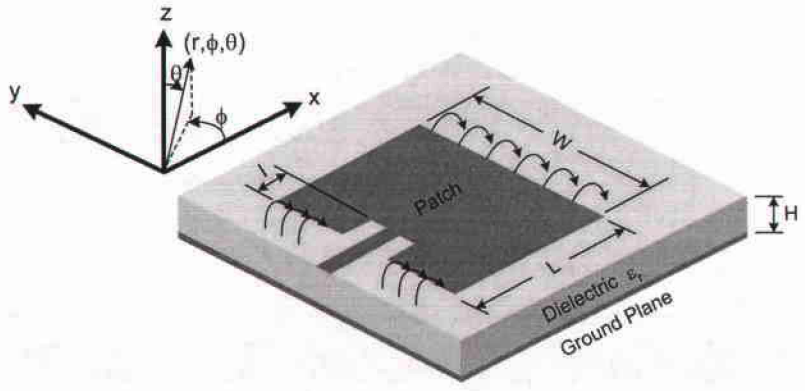

Fig. 2.8. Microstrip patch antenna with radiating-edge feed.

The patch antenna consists of a metal patch which rests on top of a dielectric substrate over a ground plane. Fig. 2.8 shows the design of a radiating-edge fed patch antenna where L and W is the length and width of the patch, respectively. Radiation is caused by the fringing electric fields at the edge of the patch, as illustrated by the arrows. As a result, the radiation efficiency is maximized for a thick substrate (large H) with a low dielectric constant (small ε_r). Since the impedance is very large at the edge of the patch, matching is usually accomplished by insetting the feed point a distance I into the patch until a 50-Ω match is achieved.

Approximate dimensions for W, L, and I, can be found in [14]. However, in practice, the final dimensions are usually determined by electromagnetic (EM) simulators. The radiation pattern of a patch antenna is fairly broad which makes it a good candidate for phased array elements. The E-plane and H-plane radiation patterns can be calculated: [15].

$$E(\theta) = \cos\left(\frac{\beta_o L}{2}\sin\theta\right) \tag{2.10}$$

$$H(\theta) = \cos\theta \frac{\sin\left[\frac{\beta_o W}{2}\sin\theta\right]}{\frac{\beta_o W}{2}\sin\theta} \tag{2.11}$$

Figs. 2.9 and 2.10 are plots of the calculated and simulated E-plane and H-plane radiation patterns for a 2.85-GHz radiating edge fed patch antenna (W = *4.11 cm*, L = *3.51 cm*) on *RT Duroid 5880* (thickness 0.7874 mm, $\varepsilon_r = 2.2$). The calculated patterns are found using (2.10)-(2.11) and are functions of the length, width, and resonant frequency of the patch. *Agilent EEsof Momentum*, an EM simulator, is used to find the simulated patterns. In addition to the length and width of the patch, *Momentum* also takes into

account the effect of the inset feeding and radiation from the 50-Ω transmission line, thus providing greater accuracy. The downside of using an EM simulator is that they can take a significant amount of time to complete, depending on the complexity of the structure being analyzed. The results of both plots agree very well between calculation and simulation and confirm that the simple equations (2.10)-(2-11) can be used to obtain a good, fast approximation.

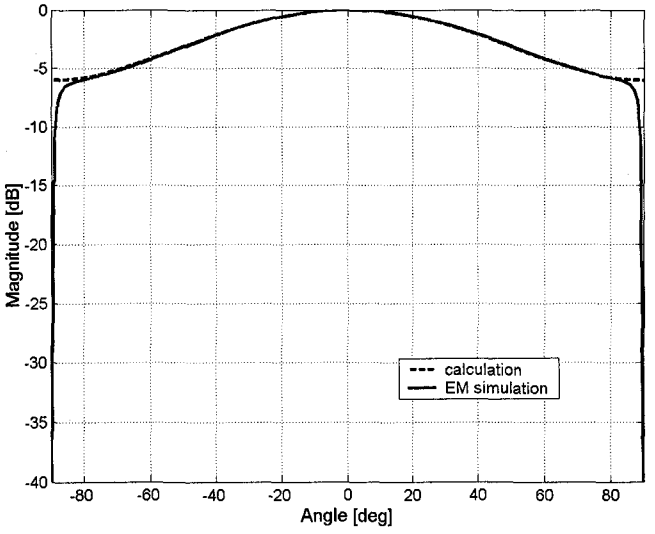

Fig. 2.9. Calculated and simulated E-plane ($\phi = 0°$) radiation pattern.

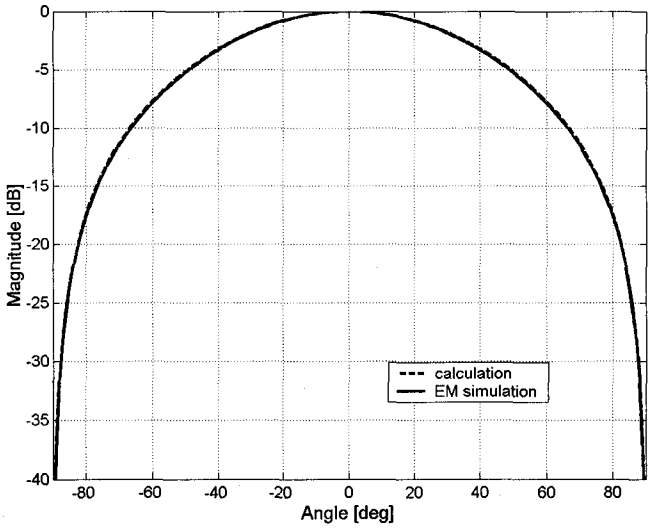

Fig. 2.10. Calculated and simulated H-plane ($\phi = 90°$) radiation pattern.

The patch antenna's fairly broad radiation pattern and low mutual coupling allows us to approximate the performance of the array, for small scanning angles (i.e. $60° \leq \phi \leq 120°$), with the results obtained for the isotropic radiator. However, since the radiation pattern of the array is a product of the element and array factor, a pointing error will result for larger scanning angles (i.e. $\phi \leq 60°$ or $\phi \geq 120°$) [16]. Fig. 2.11 shows the pointing error caused by multiplying the element pattern with the array factor pattern for a scanning angle of $\phi = 135°$.

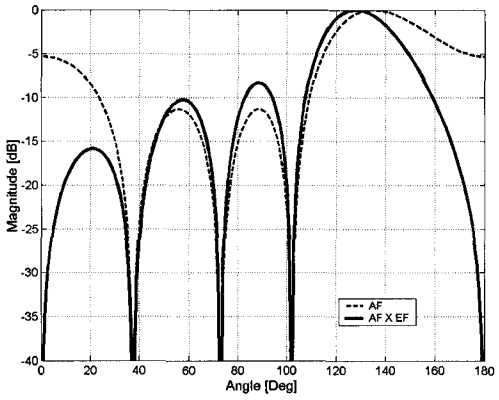

Fig. 2.11. Pointing error of phased array caused by non-isotropic element pattern of patch antenna.

2.2.3 Bistatic and Monostatic Measurements

Retrodirective arrays are characterized by their bistatic and monostatic radiation patterns. In the bistatic measurement setup shown in Fig. 2.12, the position of the RF transmitting horn in fixed while the IF receiving horn is mounted on a computer-controlled rotational arm that scans from θ= -60° to 60°.

The bistatic radar cross section (RCS) is given by (2.12).

$$\sigma_{bistatic}(\theta,\theta_0,\phi,\phi_0)=\frac{\lambda_0^2}{4\pi}G_c D_{patch}(\theta_0,\phi_0)D_{patch}(\theta,\phi)D_{array}(\theta,\theta_0,\phi,\phi_0) \quad (2.12)$$

where θ_0,ϕ_0 are the RF source angles, G_c is the circuit gain, D_{patch} is the element directivity, and D_{array} is the directivity of the array given by (2.13).

$$\begin{aligned} D_{array}(\theta,\theta_0,\phi,\phi_0) &= \frac{\left|AF(\theta,\theta_0,\phi,\phi_0)\right|^2}{U_0(\theta_0,\phi_0)} \\ &= \frac{4\pi\left|AF(\theta,\theta_0,\phi,\phi_0)\right|^2}{\int_0^{2\pi}\int_0^{\pi}\left|AF(\theta',\theta_0,\phi',\phi_0)\right|^2\sin\theta' d\theta' d\phi'} \end{aligned} \quad (2.13)$$

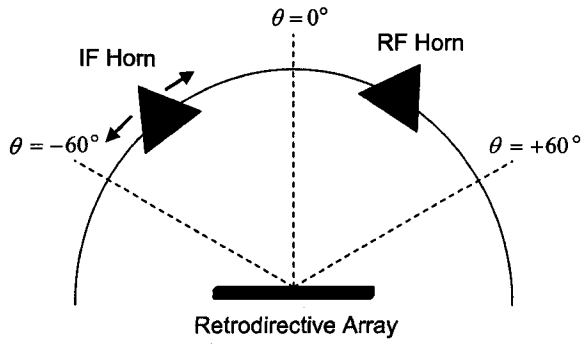

Fig. 2.12. Setup for measuring the bistatic radiation pattern.

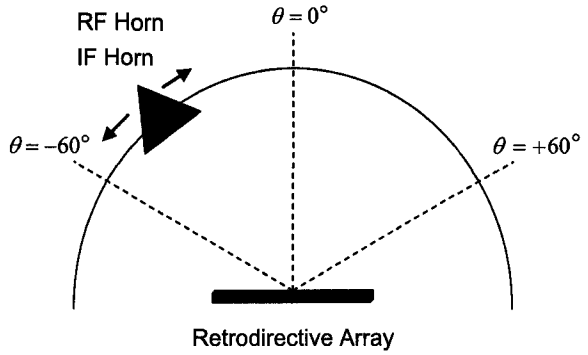

Fig. 2.13. Setup for measuring the monostatic radiation pattern.

In the bistatic measurement, the radiation pattern of the array is fixed as the position of the RF source (i.e. θ_0, ϕ_0) is fixed. This means that the integration of the array factor U_0 is constant. Therefore, the directivity of the array simply depends on the angle θ where the IF receiving horn is located at. The normalized bistatic pattern is given by (2.14).

$$\sigma'_{bistatic}(\theta,\phi)\big|_{\theta_0,\phi_0} = \frac{\left|AF(\theta,\phi)\big|_{\theta_0,\phi_0}\right|^2 D_{patch}(\theta,\phi)}{\max\left(\left|AF(\theta,\phi)\big|_{\theta_0,\phi_0}\right|^2 D_{patch}(\theta,\phi)\right)} \tag{2.14}$$

where AF is the array factor. As the array factor has the maximum value at the incoming angle of the RF signal, the main lobe of the bistatic radiation pattern should point in the direction of the source.

Another common measurement is the monostatic measurement as shown in Fig. 2.13. In this measurement, the RF and IF antennas are collocated and moved together ($\theta = \theta_0$, $\phi = \phi_0$) to measure the radiation from the array, thus the IF receiving antenna is always in the direction of the main lobe. Both the RF and IF horns are mounted on a computer-controlled rotational arm and scans together $\theta = \pm 60°$. The monostatic RCS pattern is given by (2.15).

$$\sigma_{monostatic}(\theta,\phi) = \frac{\lambda_0}{4\pi} G_c D^2_{patch}(\theta,\phi) D_{array}(\theta,\phi) \tag{2.15}$$

In the monostatic measurement, the radiation pattern varies as θ,ϕ changes. This implies that the array directivity at the peak is not constant, and it depends on the scanning angle, i.e. the position of the RF and IF horns, θ,ϕ [17], [15]. The normalized monostatic pattern is given by (2.16).

$$\sigma'_{monotatic}(\theta,\phi) = \frac{D^2_{patch}(\theta,\phi)/U_0(\theta,\phi)}{\max(D^2_{patch}(\theta,\phi)/U_0(\theta,\phi))} \tag{2.16}$$

Fig. 2.14 is the measured bistatic radiation pattern of the 4-element array shown in Fig. 2.5, where the source is positioned at 0°, -10°, -20°, and -30°. In each case, the peak of the radiation pattern is in the direction of the source, confirming proper operation of the retrodirective array. The corresponding monostatic radiation pattern is shown in Fig. 2.15. Since the IF horn and RF horn are swept together, there are no nulls in the monostatic pattern.

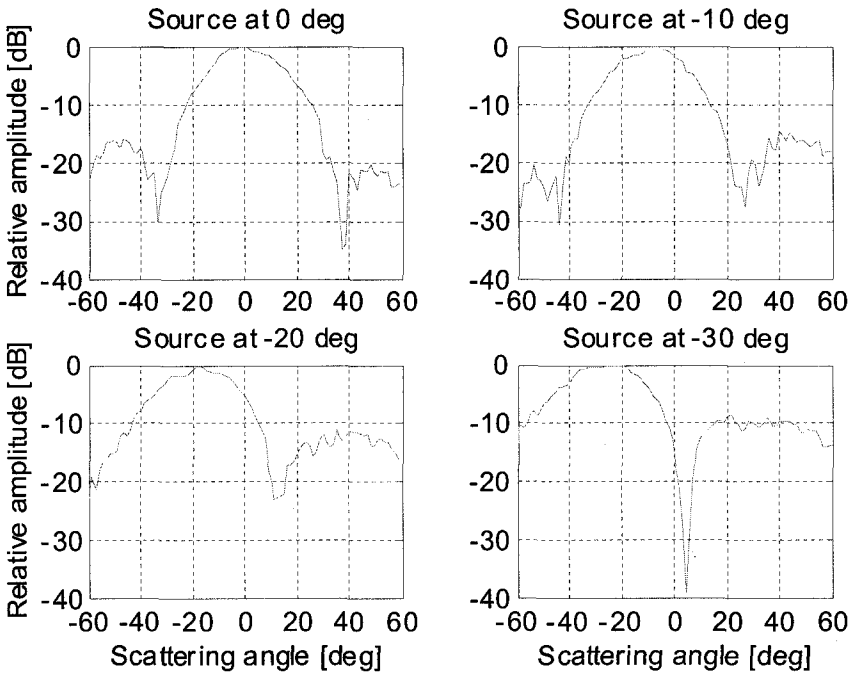

Fig. 2.14. Measured bistatic radiation patterns of the retrodirective array for RF source incident at 0°, -10°, -20°, and -30°.

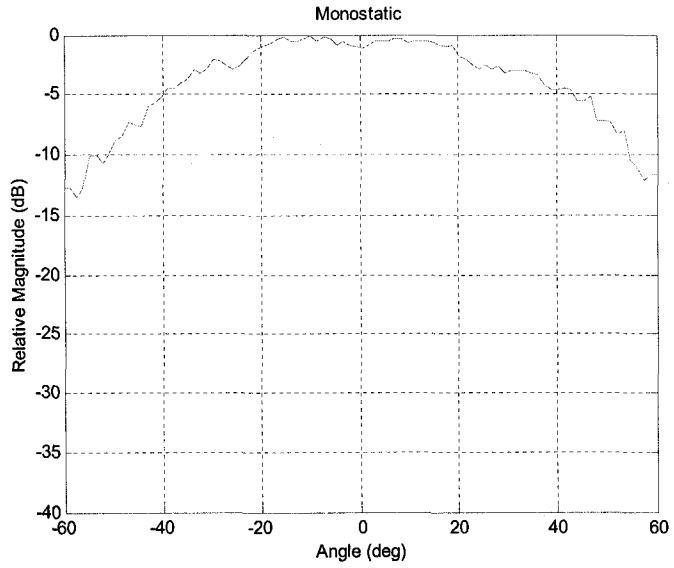

Fig. 2.15. Measured monostatic radiation pattern.

CHAPTER 3

MULTIPATH COMMUNICATIONS USING A PHASE-CONJUGATING ARRAY

3.1 Introduction

One of the major challenges in wireless systems is mitigating the fading due to multipath propagation. Not accounting for multipath may result in reduced quality and even a break in communications.

The simple solution of increasing the transmit power to overcome multipath fading comes at the cost of greatly decreasing the efficiency of the system as the multipath fading can be in the area of 40 dB. Multipath can be reduced by using antennas with tightly focused beams, signal processing, or special modulation schemes. While high-gain antennas with focused beams are useful for fixed point-to-point communications, mobile and general-purpose communication applications require antennas with wide beams or capabilities for smart beam steering. However, smart beam-steering antennas are usually complex as they require controlling electronics and computational power.

All of the methods described above are employed to *reduce* the effects of multipath. In this scheme, the multipath signals are used to *enhance* the communications in severe multipath environments. The method is based on phase-conjugating retrodirective antennas which are well-known for their self-tracking capabilities and their ability to correct for phase aberrations due to effects of disturbing and unknown media in the signal path.

Previous work involving communication with phase-conjugating antennas [18] emphasized automated beam pointing or self-steering in an environment with or without

disturbing objects, and not on the actual use of multipath propagation for communication. In [19], a retrodirective antenna was demonstrated as a multipath sensor, but not for communications. The use of multipath propagation for communications using audio waves was described in [20].

The proposed method is designed to solve problems caused by multipath propagation or disturbing objects in the signal path. Multipath propagation is used as a positive, rather than negative, contribution in the communication. In the ideal case, the fading can be completely avoided and multipath propagation only improves the radio channel.

3.2 Description of the Method

In a typical point-to-multipoint communication link, an omnidirectional base station transmits its signal in all directions. If the communication channel contains scatterers, the mobile receiving station may encounter fading due to the resulting multipath effects. Similarly, multipath affects communication from the mobile station back to the omnidirectional base station.

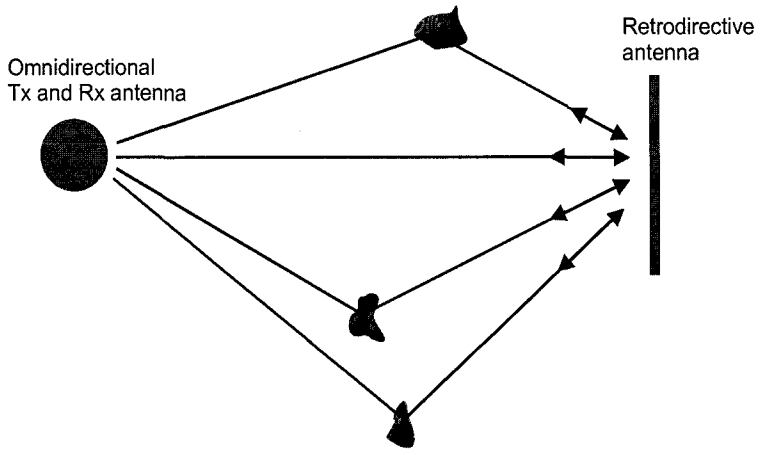

Fig. 3.1: An ideal point-to-point communication with a phase-conjugating retrodirective antenna in a multipath situation with reflecting objects.

Now consider the situation in Fig. 3.1, where the mobile station has an ideal phase-conjugating retrodirective antenna that is infinitely directive – i.e., it reflects a ray or a narrow beam only towards the direction of the incoming field. The return signal from the retrodirective antenna, which could be modulated, consists of phase-conjugated rays that add coherently at the omnidirectional source. In this way, retrodirectivity completely eliminates the fading effects of multipath propagation in the roundtrip communication link. In fact, multipath actually increases the reliability of the link since it is unlikely that all of the available paths between transmitter and receiver can be blocked simultaneously. Furthermore, since the retrodirective antenna can change its radiation pattern in real time, the scheme will still work even if there is motion of the receiver or transmitter or both.

Fig. 3.1 shows how simplex communications can be carried out from the retrodirective antenna to the wide beam antenna by modulating the reflected signal during the mixing process. For full duplex communication, both a retrodirective antenna and a wide beam antenna are needed at both ends of the link.

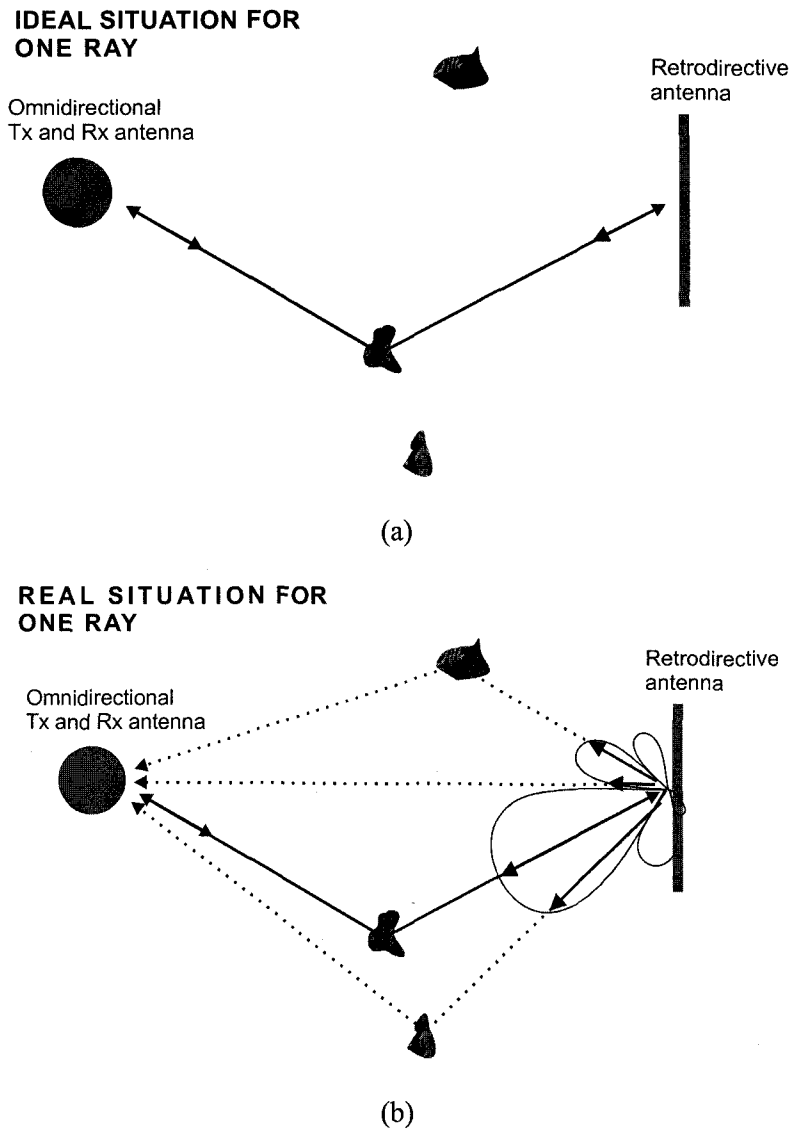

Fig. 3.2: Propagation of one ray from the omnidirectional antenna to retrodirective antenna and back in: (a) an ideal (b) a real situation.

A comparison of the ideal and practical situation is shown schematically in Fig. 3.2. For the practical case of finite antenna size, the retrodirective antenna has a finite beamwidth and sidelobes. Hence, beams reflected back from the practical retrodirective antenna not only return through the main beam path, but also through the side lobes. All of the signals corresponding to the main beam rays add up coherently whereas all the rays

created by the sidelobes have random phases and add up incoherently at the omnidirectional antenna. This limits the method in practical systems. However, reductions in deep fading and overall signal-level variations are still expected. Obviously, the situation gets more ideal as the directivity of the phase-conjugate array increases and sidelobe level decreases.

3.3 Experimental Verification

To verify the concept, an experiment was set up at 5.35 GHz, as shown in Fig. 3.3. A signal from the synthesizer is fed through a directional coupler to a horn antenna mounted on a computer controlled *x-z* stage, allowing two dimensional movements in the horizontal plane. The horn antenna is placed 1.26 m away from the retrodirective antenna and is able to move 0.74 m in the perpendicular *x*-direction, as shown in Fig 3.4. A local oscillator (LO) signal of 10.7 GHz is supplied from a synthesizer to the retrodirective antenna using a quasi-optical feed system. An LO frequency with a small offset from exactly twice the incoming signal is used so that the return signal is slightly different from the 5.351-GHz signal originally transmitted from the horn antenna. The phase-conjugating retrodirective antenna is a four-element patch antenna with FET-based mixers (Fig. 2.5) [11], with bistatic and monostatic patterns shown in Figs. 2.14 and 2.15, respectively. A mixing product with conjugated phase is reradiated by this antenna at 5.349 GHz. The returned signal at the horn is detected using the spectrum analyzer attached to the directional coupler.

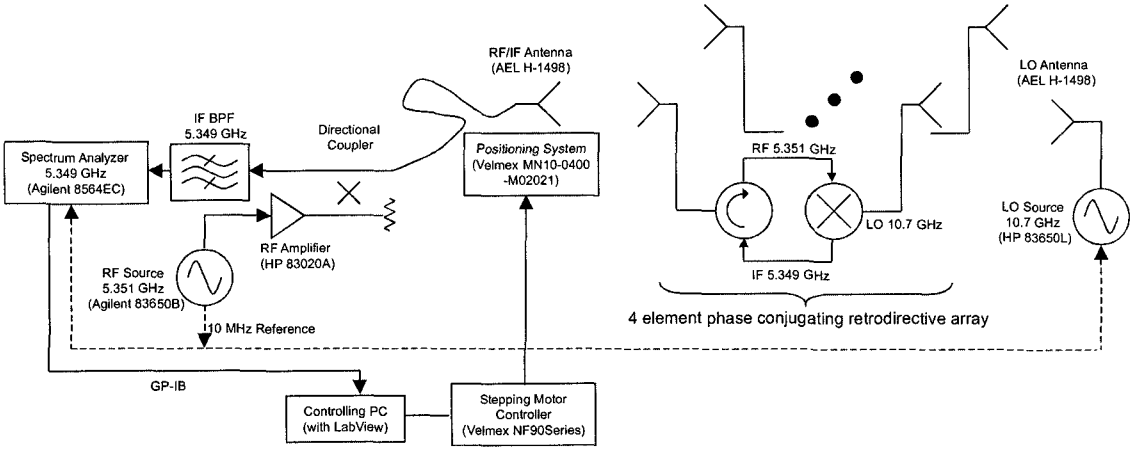

Fig. 3.3. Configuration of the automated experimental set-up at 5.35 GHz.

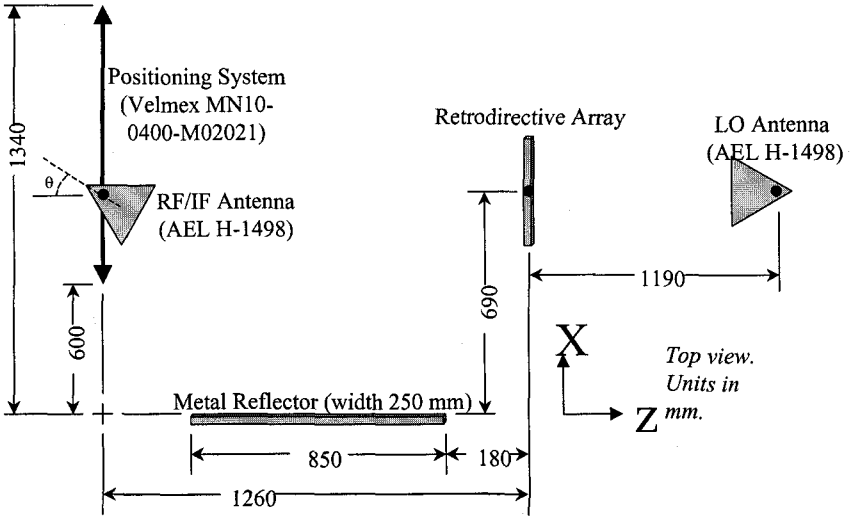

Fig. 3.4. Physical layout of the exeriment set-up.

As a baseline comparison, a passive four-element patch antenna (Fig. 3.5) with a corporate feed was used in place of the retrodirective antenna (Fig. 2.5). The far-field radiation patterns of the two antennas arrays are shown in Fig. 3.6.

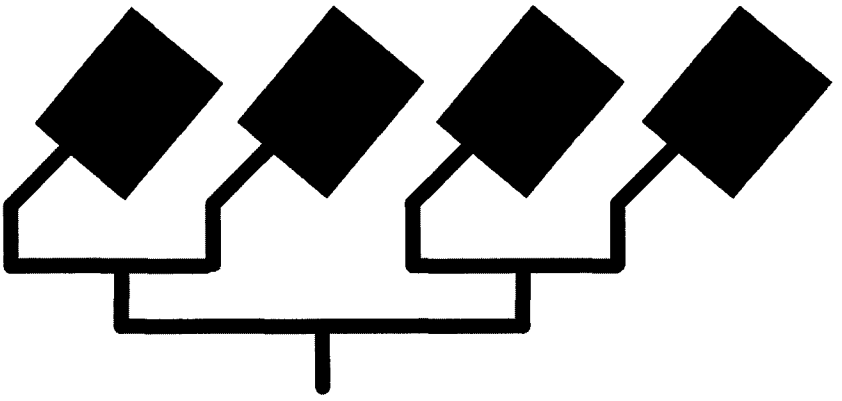

Fig. 3.5. Four-element patch antenna reference array.

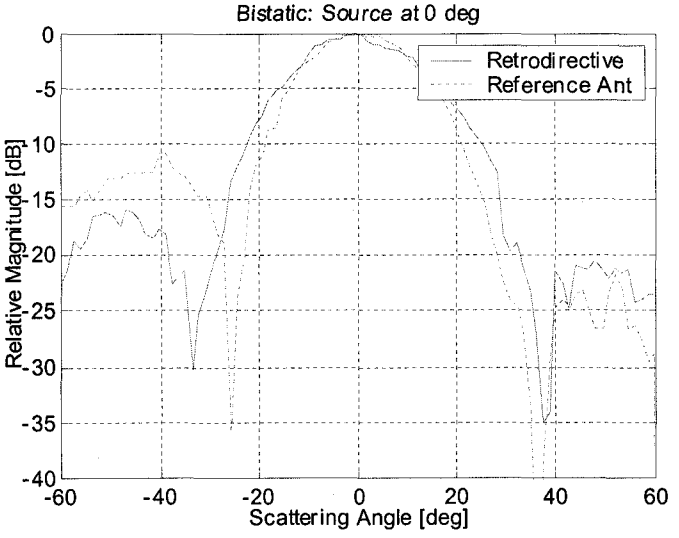

Fig. 3.6. Measured bistatic radiation pattern of the retrodirective array with RF source at 0 deg and radiation pattern of reference array.

The measurements were carried in a standard laboratory with absorber positioned in critical areas. To create a severe multipath situation, a reflective object (a metal plate) was placed in the vicinity of the antennas, as shown in Fig. 3.4. The horn antenna on the moving stage was pointed so that the direct signal and reflected (multipath) signal were comparable in amplitude. Using this same horn antenna setting and while moving it 0.74 m, the signal level was recorded for two cases: 1) the passive reference array antenna

used as a transmitting antenna and 2) the phase-conjugate antenna used to reflect the signal back. Comparison of the recorded signal level is shown in Fig. 3.7. For the reference array, the signal level varies strongly over a 40-dB range and also includes a deep dip indicating a fading point in the scan. In contrast, for the phase-conjugate antenna, the signal level varies by only 9 dB with no deep dips. This measurement shows that multipath propagation can be actually used for advantage and that the proposed method works.

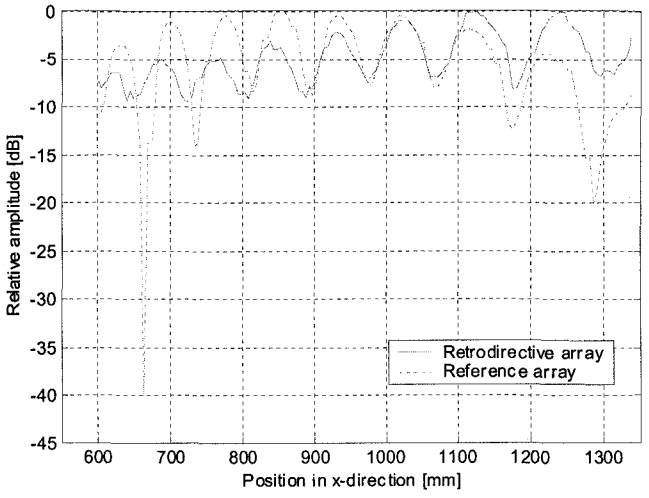

Fig. 3.7. Measured power level variation using a phase-conjugating retrodirective array and a reference array at 5.35 GHz. The source antenna is pointing towards the reflector at an angle of $\theta = 50°$.

CHAPTER 4

RETRODIRECTIVE ARRAYS FOR NON-TERRESTRIAL COMMUNICATION

4.1 Introduction

The majority of recently demonstrated retrodirective arrays are capable of retrodirectivity in one-dimension (1D). While 1D retrodirectivity may be suitable for terrestrial-to-terrestrial communications, non-terrestrial communications, such as to a plane or between two satellites, require two-dimensional (2D) retrodirectivity. Due to the added design complexities, very few 2D arrays have been published.

The Van Atta architecture is one of the traditional methods for realizing a retrodirective array, but 2D retrodirectivity is difficult to achieve since elements from opposite sides of the array must be coupled through a complicated network of overlapping lines. Two-dimensional retrodirectivity was demonstrated using four-wave mixing [21], but this architecture required four diode grids and two pumping sources.

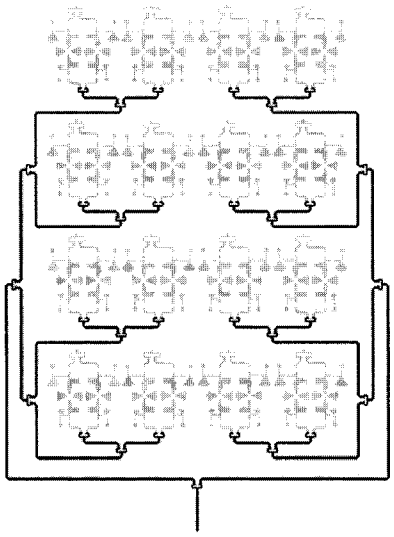

Fig. 4.1. LO feed network for a 4x4 element 2D retrodirective array [22].

For a phase-conjugating array to achieve retrodirectivity, the LO applied to each element must have the same phase. The conventional way of achieving this is to carefully design a corporate feed network so that the path lengths to each mixer are identical. However, as shown in Fig. 4.1 for a 4x4 element array [22], the feed networks becomes complicated and severely limit the maximum size of 2D arrays; in fact, only one 2D phase-conjugating array has appeared in the literature [23].

For efficient mixing, providing enough LO power to each element from a single source is challenging. Although a spatially fed LO [11] can eliminate the complex feed network, the amount of LO power delivered to the mixer is limited.

A solution to complex LO feed network and LO power requirement is to eliminate the external LO source by basing the individual phase conjugating elements on self-oscillating mixers (SOMs). A retrodirective array can then by realized by phase locking the SOM elements at the LO frequency while isolating them at the RF frequency.

Although the idea of an SOM-based retrodirective array was proposed in [24], the first such array was demonstrated in [25], but this array radiated it's LO in addition to the retrodirected IF signal and its usefulness was therefore limited. This chapter presents the first two-dimensional SOM-based array that was specifically designed for retrodirective applications.

4.2 Phase-Conjugating Circuit Based on SOMs

The self-oscillating mixer and diplexer make up the unit cell shown schematically in Fig. 4.2. The circuitry is designed such that oscillation occurs at twice the RF frequency. This will allow the lower sideband of the second order mixing product to be the phase conjugate of the RF signal. Since the size of the unit cell must be less than

$\lambda_o/2$ at the RF frequency to avoid grating lobes, the antennas are mounted on a separate layer and connected to the phase-conjugating circuit through a via.

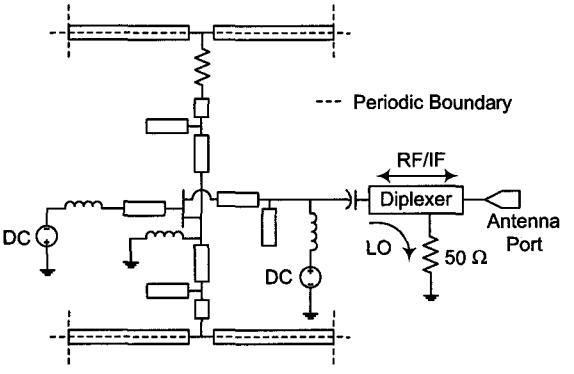

Fig. 4.2. Schematic of a phase-conjugating element using a SOM.

Phase locking of individual SOM elements is achieved by strongly coupling the source of each transistor through microstrip lines. For horizontal elements (i.e. elements parallel to the transistor's source leads), the length of the coupling line connecting each transistor's source lead is chosen to obtain a negative resistance at the desired oscillation frequency, while not exceeding the maximum unit-cell size. Vertical elements (i.e. elements parallel to the transistor's gate and drain leads) are coupled by a length of microstrip line that is a multiple of a wavelength at the LO frequency, while not exceeding the maximum unit-cell size. If the elements of the array are oscillating in phase, a virtual open is present at the periodic boundary. This allows the unit cell to be simulated by representing the microstrip lines that cross the periodic boundary as open-circuit stubs.

The unit-cell design approach is based on the assumption that all of the elements oscillate in phase [26]. However, in an array containing multiple elements, it is possible for other modes of oscillation to occur. A method of analyzing different oscillation modes of a one-dimensional array of strongly coupled oscillators is presented in [27].

Suppression of the unwanted modes is achieved by introducing a resistor at the midpoint of the lines coupling adjacent elements. A similar problem where adjacent horizontal elements would lock 180° out of phase was encountered during initial measurement of the prototype. By simulating a high-impedance voltage source at the LO frequency that is connected to the source of the transistor of each phase-conjugating element, we can obtain the voltage standing wave along different points of the coupling lines. If the sources are configured so that both the in-phase and 180° out-of-phase modes of oscillation are simulated, the results can be compared and a solution to attenuate the out-of-phase mode can be found. Introducing a resistor on the horizontal coupling line, before the intersection of the vertical coupling line as shown in Fig. 4.2 does little affect to the in-phase mode, since it is at the virtual open point. However, simulation shows that a resistor at this position attenuates the 180° out-of-phase mode.

While the elements of the array are strongly coupled at the LO frequency, a retrodirective array requires that each element be isolated at the RF/IF frequency. Single-stub RF band-stop filters are employed on each side of the transistor on the horizontal coupling lines to provide isolation between adjacent elements at the RF/IF frequency.

The oscillation frequency of the self-oscillating mixer is determined by optimizing the length of the open-circuit stub attached to the transistor's gate in conjunction with the matching network at the drain to achieve a negative resistance of -150 Ω in accordance to the one-third rule [28].

For the mixing operation, the RF and IF is applied and extracted from the drain of the transistor. A diplexer comprised of single-stub band-stop filters is inserted to reduce unwanted LO radiation by isolating the antenna port from the LO termination. At

the LO frequency, the output port of the SOM only sees the 50-Ω load while only the antenna is visible at the RF/IF frequency.

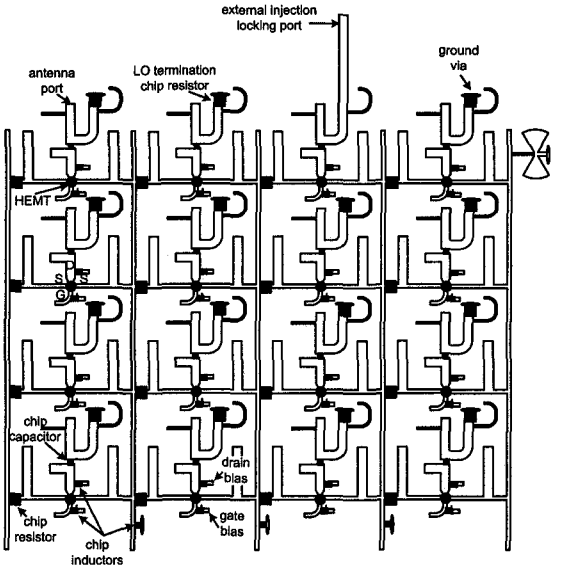

Fig. 4.3. 4 x 4 element phase-conjugating circuit using SOMs.

The prototype 16-element phase-conjugating SOM array is shown in Fig. 4.3. The circuit is fabricated on *RT/duroid* 5880 substrate (thickness 0.7874 mm, ε_r=2.2). The active devices are Agilent ATF-36077 ultra low noise pseudomorphic high electron mobility transistors (pHEMT). Gate and drain biasing is applied through chip inductors while chip capacitors provide DC blocking. SMA connectors are mounted on the ground plane side of the substrate through drilled holes to allow a connection to the RF/IF port of the diplexer. This configuration simplifies testing of individual phase-conjugating elements. A SMA connector is also mounted to one element at the edge of the array in place of the LO termination to serve as an external injection locking port. Unwanted modes of oscillation are suppressed by inserting a 50-Ω resistor on the horizontal coupling line as depicted in Fig. 4.2. This resistor value was chosen based on availability, but any reasonable value should be appropriate since the in-phase mode is unaffected by

this resistor. All vertical coupling lines were DC grounded to negate the effect of the mode-stabilizing resistance on the transistor biasing.

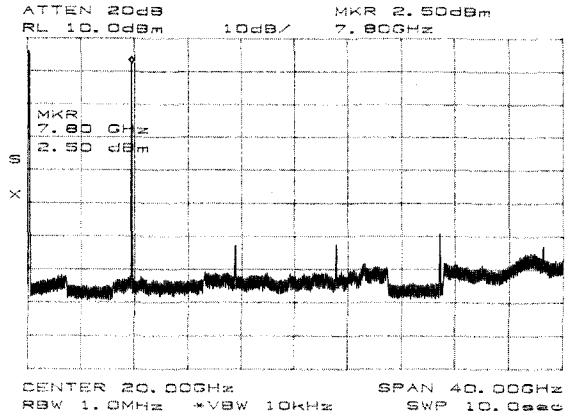

Fig. 4.4. LO spectrum generated by the SOM circuit.

For proper operation of the SOM array, the SOMs have to be turned on at the same time. This is achieved by using a common DC supply for all the SOMs. The transistors are biased at class-A. The circuit is optimized so that it oscillates at 8.0 GHz. Fig. 4.4 shows the measured spectrum of the oscillation signal taken at the external injection locking port. The measurement shows that the SOM elements are phased locked with a fundamental oscillation frequency of 7.80 GHz. Discrepancies between the simulated and measured oscillation frequency is due to the insertion of the chip resistor used for mode stabilization. While an ideal resistor of zero length would not affect the in-phase mode, the resistor used has a finite length that was not compensated for in this prototype. At the fundamental frequency, an oscillation power of 3.8 dBm is measured for a single SOM element.

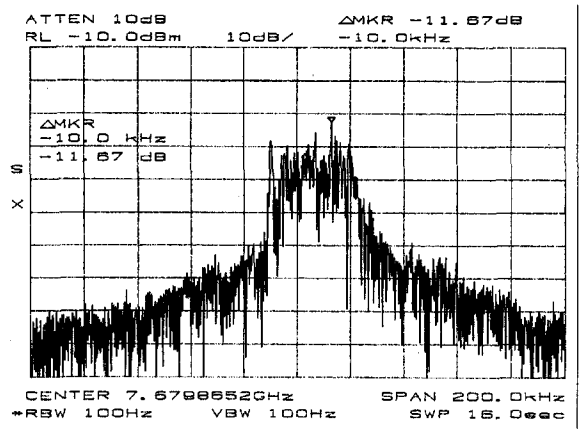

Fig. 4.5. Spectrum of LO without external injection locking.

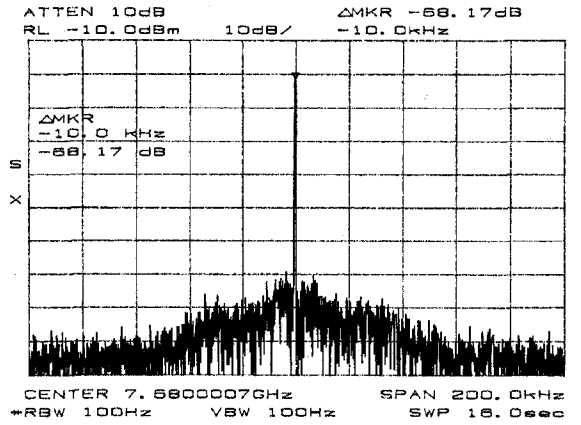

Fig. 4.6. Spectrum of LO with external injection locking.

To evaluate the effects of external injection locking, the phase noise of the oscillation signal is measured. The injection-locking signal is applied at the edge of the array through the external injection-locking port while the LO leakage signal is monitored through the RF/IF port at the opposite side of the 16-element array. A HP 83650L signal generator is used as the injection locking source since it is capable of providing a low phase-noise signal of -80 dBc/Hz at 10 kHz offset. Fig. 4.5 shows the phase noise of the oscillation signal without external injection locking to be -11.7 dBc/Hz at 10 kHz offset. When a -10 dBm external injection locking signal at 7.680 GHz is

applied, the phase noise reduces to -68.2 dBc/Hz at 10 kHz offset as shown in Fig. 4.6. Besides reducing the LO phase noise, the injection-locking signal could also be used as a source for frequency or phase modulation schemes.

Next, mixing performance is evaluated by applying an external RF signal to the SOM circuit through a directional coupler [29]. The phase-conjugated IF signal is measured using a spectrum analyzer from the coupled port of the directional coupler. At an RF frequency of $f_{LO}/2$, the measured conversion gain is -20.6 dB. Low conversion gain is expected since the SOM was only optimized for oscillation according to the one-third rule without taking the mixing performance into account.

For an array of phase-conjugating elements to properly function as a retrodirective array, each element must be isolated from one another. The RF isolation between elements is measured by injecting a RF signal into an element and measuring the coupled signal at an adjacent element. At a RF frequency of 3.84 GHz, the RF isolation between adjacent horizontal elements is 17.9 dB and 22.2 dB between adjacent vertical elements.

4.3 Two-Dimensional Retrodirective Array

A 4x4 array of radiating-edge fed patch antennas, shown in Fig. 4.7, is fabricated such that the element spacing is equal to the phase-conjugating array unit cell. At a RF frequency of 3.840 GHz, the element spacing in the H-plane is 3.48 cm (0.464 λ_o) and 2.90 cm (0.386 λ_o) in the E-plane. *RT/duroid* 5880 (thickness 0.7874 mm, ε_r=2.2) is the substrate used for the patch-antenna array. SMA connectors are mounted on the ground plane side of the substrate through drilled holes to allow a connection to be made to

individual patch antennas. This configuration allows testing and tuning of individual antenna elements and facilitates easy interfacing with the phase-conjugating circuit.

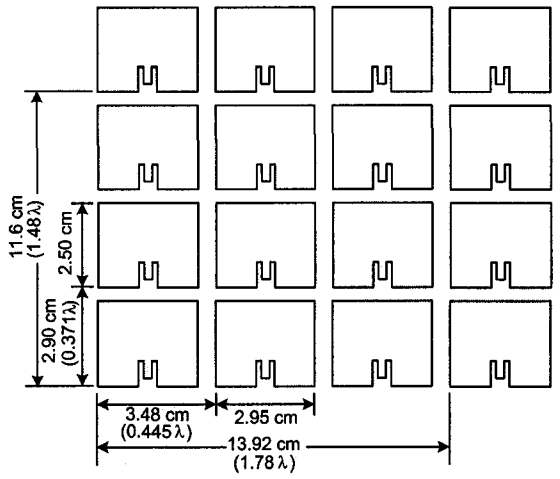

Fig. 4.7. 4 × 4 element patch antenna array.

Using the coordinate system shown in Fig. 4.8, the operation of the 2D array is confirmed with a series of bistatic and monostatic radiation patterns. Figs. 4.9 and 4.10 show the measured and theoretical bistatic radiation patterns and the monostatic radiation pattern in the E-(ϕ = 0°) and H-(ϕ = -90°) planes. The bistatic radiation patterns are measured with RF sources at θ = 0°, θ = -15°, and θ = +30°. The theoretical patterns are obtained based on (2.14) and (2.16). The measured bistatic and monostatic radiation patterns show retrodirectivity in both of the principle planes and confirm the operation of the 2D prototype.

A second confirmation can be obtained by taking a measurement along a plane, different from the principle E-plane and H-plane. Unique only to a 2D retrodirective array, the success of this measurement requires the proper operation of elements in both planes. Fig. 4.11 shows the measured bistatic radiation patterns in the ϕ = -45° plane with

RF sources at θ = 0°, θ = -15°, and θ = +30°, and the monostatic radiation pattern. The results confirm operation of the 2D prototype.

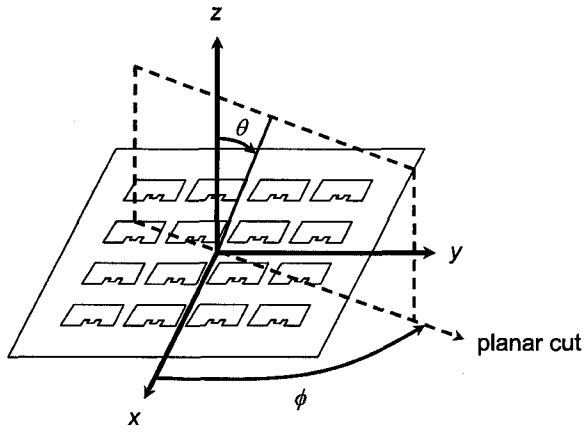

Fig. 4.8. Coordinate system used for radiation pattern measurements.

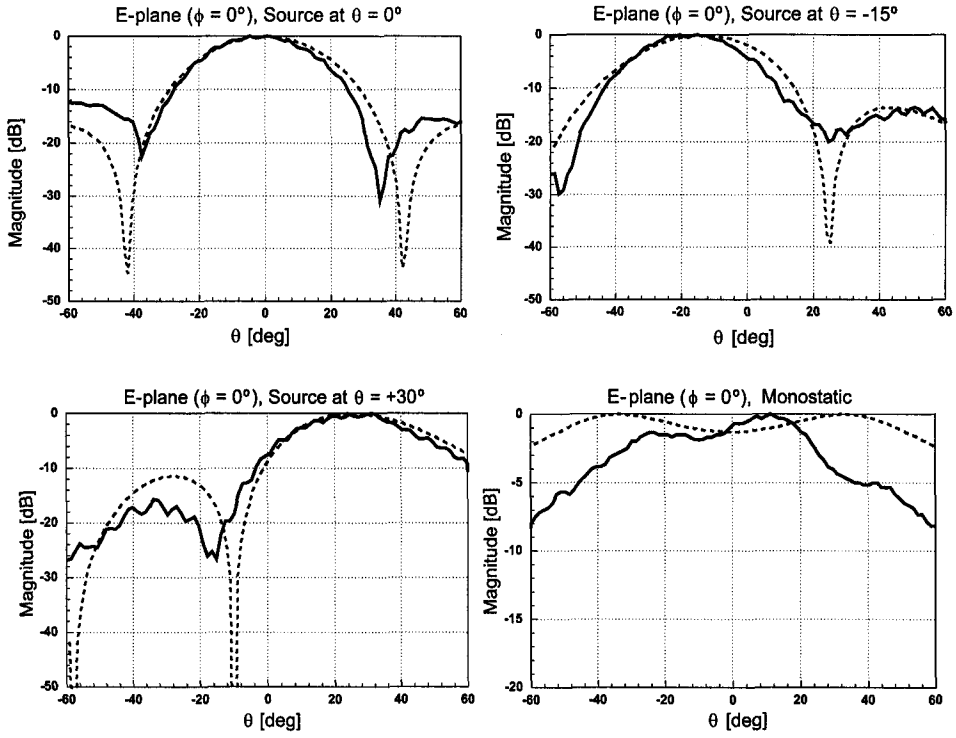

Fig. 4.9. E-plane (ϕ = 0°) bistatic radiation patterns for scattering angles of θ = 0°, θ = -15°, and θ = +30° and monostatic radiation pattern.

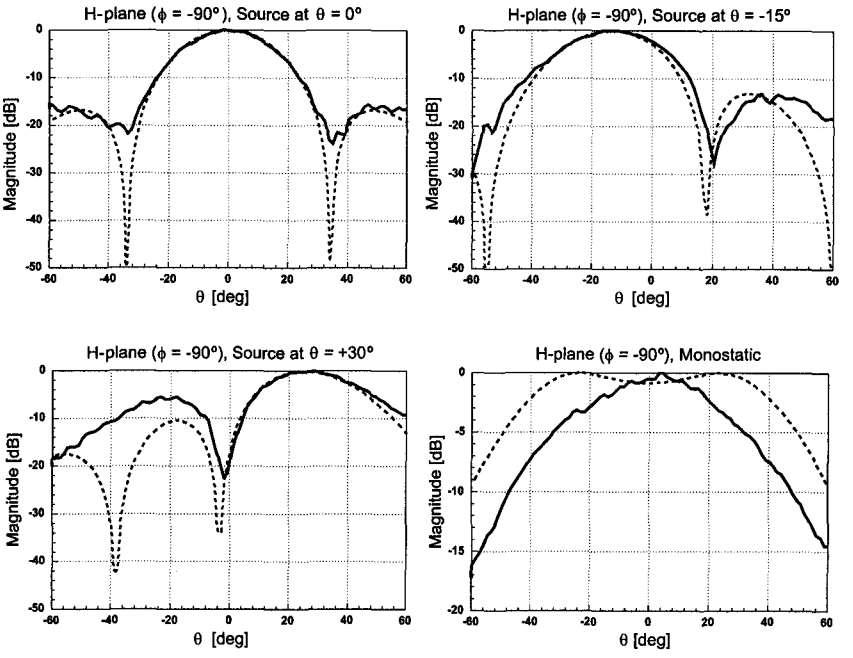

Fig. 4.10. H-plane (ϕ = -90°) bistatic radiation patterns for scattering angles of θ = 0°, θ = -15°, and θ = +30° and monostatic radiation pattern.

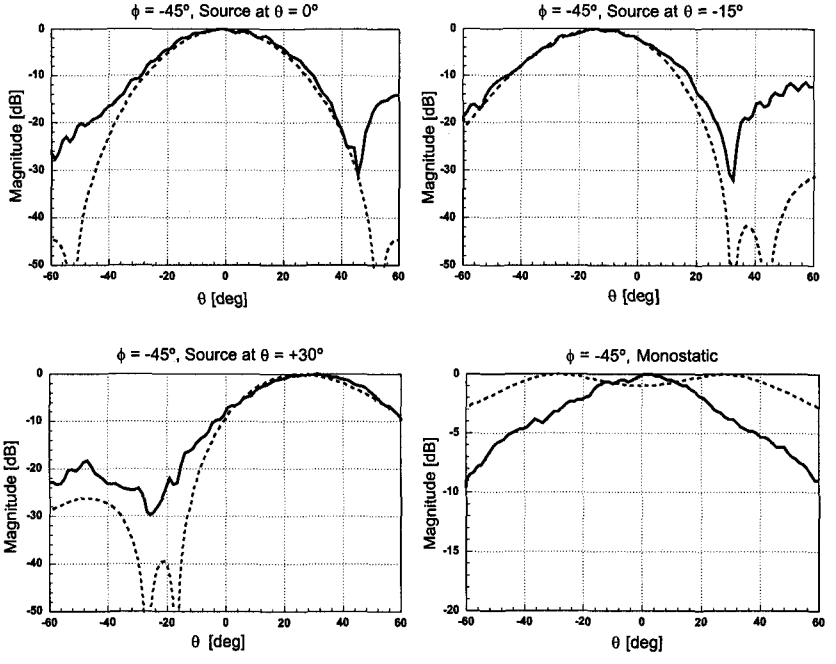

Fig. 4.11. ϕ = -45° bistatic radiation patterns for scattering angles of θ = 0°, θ = -15°, and θ = +30° and monostatic radiation pattern.

CHAPTER 5

RETRODIRECTIVE ARRAYS FOR SMALL-SATELLITE NETWORKS

5.1 Introduction

Self-steering retrodirective arrays for picosatellite applications permit secure crosslink communications between satellites moving randomly in space [30] without the added complexities of digital signal processing. Compared to omnidirectional antennas, the higher directivity associated with retrodirective arrays not only improves network security, but also improves the communication link efficiency by minimizing power consumption.

The most popular method of achieving retrodirectivity is to mix the incoming RF signal with an LO signal at twice the RF frequency. However, this approach requires a high frequency, high power LO source which puts a strain on the limited DC power budget of small satellites. The subharmonic mixing approach is well suited for high-frequency systems as it eliminates the need for a high-frequency LO [31], [32]. Previously reported phase-conjugators based on the subharmonic mixing all use third-order mixing ($f_{IF} = 2f_{LO} - f_{RF}$), allowing the use of an LO in the same band as the RF. However, this approach suffers from large LO leakage as the fundamental LO frequency overlaps the RF, and cannot be filtered.

This chapter presents the results for an array specifically designed for picosatellite crosslink applications. To accommodate for randomly oriented satellites in space, the array presented here demonstrates two-dimensional steering with circular polarization. As mentioned in Chapter 4, only a limited number of papers on two-

dimensional retrodirective arrays have been reported in the literature [33]. The novel use of fifth-order quadruple subharmonic mixing using anti-parallel diodes allows for improved LO/IF isolation and relaxes the requirement on the local oscillator frequency, compared to the conventional second-order and third-order subharmonic approaches.

5.2 Design

5.2.1 Design Constraints

Although retrodirective technology has been around since the 1960s, designing for space applications presents new challenges. First, the zero-gravity, free-floating nature of the satellites necessitates two-dimensional tracking – and therefore a two-dimensional retrodirective array. Secondly, since the satellites are too small to have attitude control systems, it is impossible to know the orientation of each satellite. The antennas will therefore have to provide circular polarization to allow signal reception and prevent polarization mismatch regardless of each satellite's orientation with respect to the other.

The array in this work is designed for 10.5 GHz – a frequency that not only minimizes the array size to fit within the 10 x10 x 15 cm form factor, but also is an allocated frequency in the amateur radio satellite band.

5.2.2 Mixer

The quadruple subharmonic mixing approach was adopted in our system and is described here:

$$V_{IF} \propto \left[V_{LO}\cos(\omega_{LO}t)+V_{RF}\cos(\omega_{RF}t+\varphi)\right]^5+\ldots$$

$$V_{IF} \propto \frac{5}{16} V_{LO}{}^{4} V_{RF} \cos(4\omega_{LO} t - \omega_{RF} t - \varphi) + \ldots \tag{5.1}$$

If $2\omega_{LO} = \omega_{RF}$, the right hand side of (5.1) becomes the phase conjugate of the incoming RF signal. Therefore, by using the fifth-order mixing product ($f_{IF} = 4f_{LO} - f_{RF}$), the LO frequency requirement is reduced from twice (second-order mixing) to half the RF frequency. Anti-parallel diodes suppress even order harmonics, including the second harmonic of the LO, which would be at the same frequency as the RF. Other odd order mixing terms can be easily filtered out.

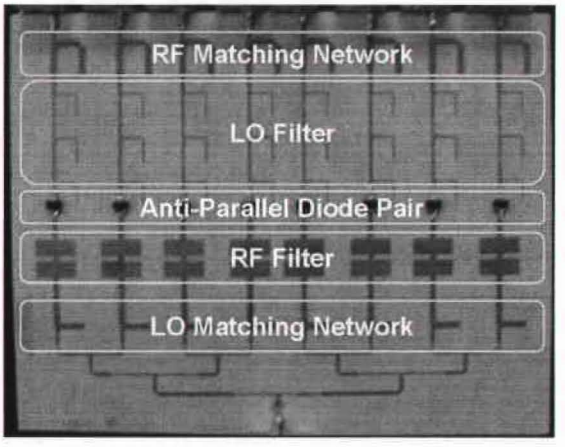

Fig. 5.1. The phase conjugating circuit consisting of series-pair diodes connected in an anti-parallel configuration, LO and RF matching networks, and bandstop filters at the RF and LO frequencies.

Fig. 5.1 shows the phase conjugating circuit, which uses Agilent HSMS-8202 series-pair diodes connected in an anti-parallel configuration. The microstrip filters and matching networks are printed on Rogers TMM4 substrate (ϵ_r=4.5, h=0.0381 cm). The measured isolation between the IF and fundamental LO is 65 dB. The rejection of the LO second harmonic is 55 dB, which is superior to third-order mixing, and the measured conversion loss of the subharmonic mixer is 26 dB.

5.2.3 Antenna Element and Array

The antenna element is a square microstrip patch, mitered at opposite ends to achieve two different resonant modes; circular polarization is achieved when the two modes are orthogonal to each other and 90° out of phase (Fig. 5.2). The antenna is fabricated on Rogers TMM3 substrate (ϵ_r=3.27, h=0.0635 cm).

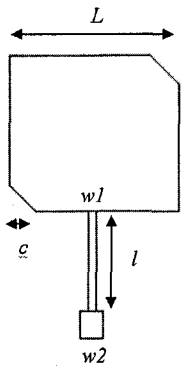

Fig. 5.2 Patch antenna element with dimensions L = 0.762 cm, c = 0.102 cm, $w1$ = 0.0457 cm, l = 0.541 cm, $w2$ = 0.150 cm.

Significant retrodirectivity requires an array of at least four elements per dimension. Conventionally, this is achieved with a 4 x 4 array layout. To reduce circuit size and required feed power, a cross-shaped array consisting of four elements in two orthogonal dimensions was used instead, reducing the amount of elements from 16 for the conventional array to eight elements. The array spacing is 0.484λ = 1.383 cm between elements (Fig. 5.3).

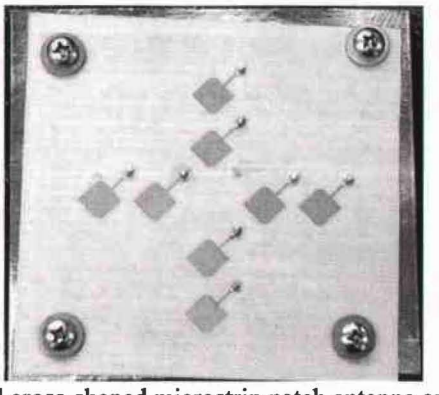

Fig. 5.3. Circularly polarized cross-shaped microstrip patch antenna array at 10.5 GHz.

5.3 Experimental Results

Fig. 5.4 shows the bistatic radiation pattern of the 2D quadruple subharmonic retrodirective array prototype. The following frequencies were used during measurement: LO signal of 5.2375 GHz (fourth subharmonic of 20.95 GHz), RF signal of 10.45 GHz, and IF signal of 10.5 GHz. To ensure that 2D retrodirectivity is achieved, the measurements are taken along the 45° cut of Fig. 5.3, *not* along the 0° or 90° axes on which the linear arrays are aligned. The measurements confirm retrodirectivity for source angles of 0°, +20°, and -20°. The polarization ellipse was also measured and found to be 5.5 dB.

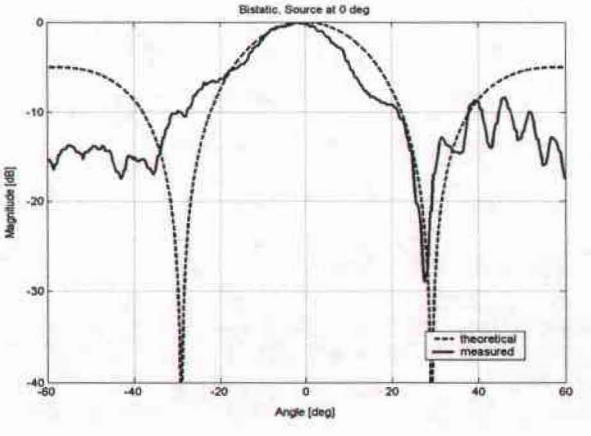

(a)

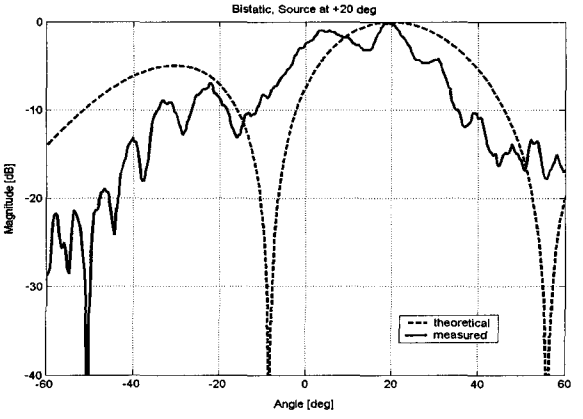

(b)

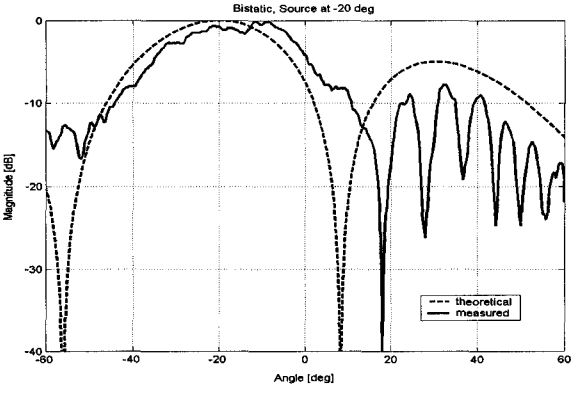

(c)

Fig. 5.4 Measured and theoretical bistatic radiation pattern with the source positioned at (a) 0°, (b) +20°, and (c) -20°.

CHAPTER 6

CONCLUSIONS AND FUTURE WORK

6.1 Conclusions

This thesis discussed the benefits of using self-steering arrays in wireless communication systems and presented several new advances in the designs of retrodirective arrays. Retrodirective arrays continue to be a hot area of research because they are able to perform complicated tasks, such as automatic beam steering and multipath compensation, using a very simple circuit.

The method of using a phase-conjugating retrodirective array to compensate for multipath was described and verified in Chapter 3. Since multipath propagation can cause fading, and potentially even a complete break in the communication link, compensation for multipath not only improves the reliability of the system, but also increases the overall efficiency since less transmit power is required to maintain a stable link. Using a four-element phase-conjugating array, a 31-dB improvement was experimentally measured at 5.35 GHz. The performance can be further increased by increasing the number of array elements.

To provide two-dimensional retrodirectivity for terrestrial to space or space to space applications, a two-dimensional retrodirective array was developed. Chapter 4 shows the design for one of the first four-by-four element, two-dimensional retrodirective arrays. Minimizing the size of the design to a half-wavelength by half-wavelength unit cell was accomplished by replacing the heterodyne mixers of a phase-conjugating array, along with the complicated feed network, with an array of phase locked self-oscillating mixers. Correct operation of the self-oscillating mixer array was ensured by suppressing other out-of-phase modes with a resistor inserted in the coupling lines. An external

injection locking source reduced the overall phase noise of the array while providing a source of modulation.

Chapter 5 presented a 10.5-GHz retrodirective array for picosatellite networks. Since the space constraints of picosatellites make it almost impossible to incorporate the more complicated, DSP based smart antenna, retrodirective arrays are the preferred solution. Quadruple subharmonic mixing was shown to be an effective means of achieving phase conjugation when a high frequency LO is difficult to implement. An 8-element two-dimensional retrodirective array was fabricated with circularly polarized patch antennas.

6.2 Suggestions for Future Work

One of the practical limitations of almost all the retrodirective arrays that appear in literature is the power dependence of the retrodirected signal to the interrogating signal. Since the signal must travel a distance, R, to the retrodirective array and back, the power level of the signal will be proportional to approximately $1/R^4$ (Fig. 6.1a). In most cases, the cost of generating a powerful interrogating signal to overcome the extra $1/R^2$ loss outweighs the added gain of the array. This is especially true for a small satellite application where available power is severally limited. By decoupling the retrodirective signal from the interrogating signal, a strong and constant retrodirected power level will be transmitted back to the source (Fig. 6.1b). This will reduce the loss of the system with the power of the signal now proportional to approximately $1/R^2$.

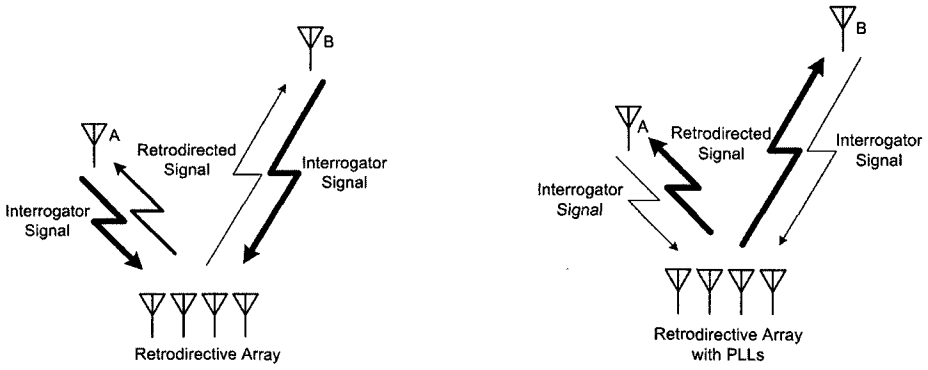

Fig. 6.1. Relative power levels, represented by thickness of arrows (*i.e.* thicker arrow represents stronger signal), of interrogator and retrodirected signal for a retrodirective array (a) conventional retrodirective array, (b) retrodirective array where the interrogator and retrodirective signal is decoupled.

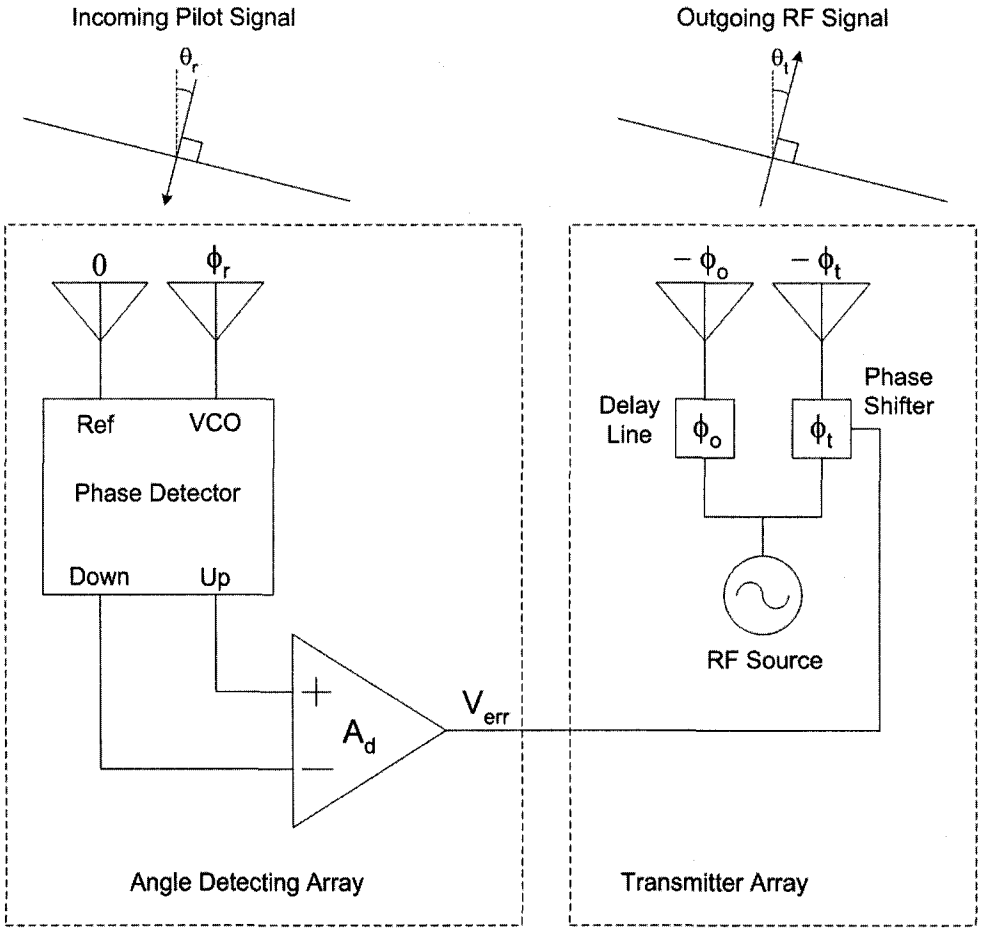

Fig. 6.2. Retrodirective array using phase detection and shifting.

The proposed design of the retrodirective array, capable of maintaining a constant transmit power is shown in Fig. 6.2. Unlike the conventional Van Atta and heterodyne type phase conjugating designs, the proposed design uses a phase detector to detect the incoming angle of the interrogating signal. The resultant error voltage is fed to a phase shifter which directs the beam of the transmitting array back in the direction of the source. The power of the transmitting signal is determined by the power of the RF source and is completely independent of the power from the interrogator.

REFERENCES

[1] "Nokia annual figures." Retrieved July 21, 2004 from, www.nokia.com.

[2] "US frequency allocation chart." Retrieved July 21, 2004 from the *National Telecommunications and Information Administration Office of Spectrum Management*, http://www.ntia.doc.gov/osmhome/allochrt.html.

[3] S.-S. Jeng, G. T. Okamoto, G. Xu, H.-P. Lin, W. J. Vogel, "Experimental evaluation of smart antenna system performance for wireless communications," *IEEE Trans. Antennas Progagat.*, vol. 46, pp. 749-757, June 1998.

[4] C. Y. Pon, "Retrodirective array using the heterodyne technique," *IEEE Trans. Antennas Propagat.*, vol. 12, pp 176-180, Dec. 1964.

[5] H. Heidt, J. Puig-Suari, A. S. Moore, S. Nakasuka, R. J. Twiggs, "CubeSat: a new generation of picosatellite," in *Proc. of the 14th Annual AIAA/USU Conference on Small Satellites*, Logan, UT, Aug. 2001.

[6] J. D. Kraus, *Antennas*. New York: McGraw-Hill, Inc., 1988.

[7] L. C. Van Atta, "Electromagnetic Reflector," U.S. Patent #2,908,002, Oct. 6, 1959.

[8] N. B. Buchanan, T. Brabetz, and V. F. Fusco, A 62/66 GHz frequency offset retrodirective array, *IEEE MTT-S Int. Microwave Symp. Dig.*, Seattle, WA, 315–318, 2002.

[9] S. A. Maas, *Nonlinear Microwave and RF Circuits*, Norwood, MA: Artech House, Inc., 2003.

[10] R. Y. Miyamoto, Y. Qian, and T. Itoh, "A retrodirective array using balanced quasioptical FET mixers with conversion gain," *IEEE MTT-S Int. Microwave Symp. Dig.*, Anaheim, CA, pp. 655-658, June 1999.

[11] W. E. Forsyth and W. A. Shiroma, "A retrodirective antenna array using a spatially fed local oscillator," *IEEE Trans. Antennas Propagat., Special Issue on Wireless Information Technology and Networks*, vol. 50, pp. 638–640, May 2002.

[12] L. D. DiDomenico and G. M. Rebeiz, Digital communications using self-phased arrays, *IEEE Trans. Microwave Theory Tech.*, vol. 49, pp. 677 -684, 2001.

[13] M. Iskander, *Electromagnetic Fields and Waves*. Prospect Heights, Illinois: Waveland Press, Inc., 2000.

[14] C. Balanis, *Antenna Theory Analysis and Design*. New York: John Wiley & Sons, Inc., 1997.

[15] W. Stutzman, G. Thiele, *Antenna Theory and Design*. New York: John Wiley & Sons, Inc., 1998.

[16] S. L. Karode and V. F. Fusco, "Self-tracking duplex communication link using planar retrodirective antennas," *IEEE Trans. Antennas Propagat.*, Vol. 47 No. 6, pp. 993-1000, June 1999.

[17] R. C. Hansen, Phased array antennas, New York: John Wiley and Sons, 1997.

[18] Y. Chang, H. R. Fetterman, I. L. Newberg, and S. K. Panaretos, "Microwave phase conjugation using antenna arrays," *IEEE Trans. Microwave Theory Tech.*, vol. 46, no. 11, pp. 1910-1919, Nov 1998.

[19] S. L. Karode and V. F. Fusco, "Use of an active retrodirective antenna as a multipath sensor," *IEEE Microwave and Guided Wave Letters.*, vol. 7, no. 12, pp. 399-401, Dec 1997.

[20] M. Fink, "Time-reversed acoustics," Scientific American, pp. 91-97, Nov 1999.

[21] W. Ding, S-T. C. Lei, and M. P. DeLisio, "A retrodirective diode grid array using four-wave mixing," *2001 IEEE MTT-S Int. Microwave Symp. Dig.*, pp. 1851-1854, Phoenix, AZ, May 2001.

[22] R. Y. Miyamoto, "Adaptive RF Front-Ends for Digital Wireless Communications," PhD dissertation, University of California, Los Angeles, 2002.

[23] C. W. Pobanz, "Time-Varying Active Antennas: Circuits and Applications," PhD dissertation, University of California, Los Angeles, 1997.

[24] S. C. Yen and T. H. Chu, "Phase conjugation array using subharmonically injection locked self-oscillating mixers," in *2001 IEEE AP-S International Symp Dig.*, pp. 692-695, Jul. 2001.

[25] D. M. K. Ah Yo, W. E. Forsyth, and W. A. Shiroma, "A 360° retrodirective self-oscillating mixer array" in *IEEE MTT-S Int. Microwave Symp. Dig.*, Boston, MA, pp. 813-816, June 2001.

[26] S. Kawasaki and T. Itoh, "Quasi-optical planar arrays with FETs and slots," *IEEE Trans. Microwave Theory Tech.*, vol. 41, no. 10, pp. 1838-1844, Oct. 1993.

[27] S. Nogi, J. Lin, and T. Itoh, "Mode analysis and stabilization of a spatial power combining array with strongly coupled oscillators," *IEEE Trans. Microwave Theory Tech.*, vol. 41, no. 10, pp. 1827-1837.

[28] G. Gonzalez, Microwave transistor amplifiers analysis and design, New Jersey: Prentice-Hall, 1997.

[29] R. Y. Miyamoto, Y. Qian, and T. Itoh, "An active retrodirective transponder for remote information retrieval-on-demand," *IEEE Trans. Microwave Theory Tech.*, vol. 49, no. 9, pp. 1658-1662, Sep. 2001.

[30] B. T. Murakami, M. A. Tamamoto, A. T. Ohta, G. S. Shiroma, R. Y. Miyamoto, and W. A. Shiroma, "Self-steering antenna arrays for distributed picosatellite networks," in *Proc. of the 17th Annual AIAA/USU Conference on Small Satellites,* Logan, UT, Aug. 2003.

[31] J. Y. Park, K. M. K. H. Leong, G. R. Kim, J. I. Choi, and T. Itoh, "Active Retrodirective Array with Subharmonic Phase Conjugation Mixers," in *Proc. of the 2003 Asia-Pacific Microwave Conference*, Seoul, Korea, Nov. 2003.

[32] T. Brabetz, V. F. Fusco, and S. Karode, "Balanced Subharmonic Mixers for Retrodirective-Array Applications," *IEEE Trans. Microwave Theory Tech.*, vol. 49, Mar. 2001.

[33] G. S. Shiroma, R. Y. Miyamoto, and W. A. Shiroma, "A 16-element two-dimensional active self-steering array using self-oscillating mixers," *IEEE Trans. Microwave Theory Tech.*, vol. 15, pp. 2476-2482, Dec. 2003.